Eur J Pharmacol. 2021; 902:174091.
doi: 10.1016/j.ejphar.2021.174091.
Accepted 31 Mar 2021. Online: 16 Apr 2021. Published 5 July 2021

Mechanistic evaluation of a novel cyclohexanone derivative's functionality against nociception and inflammation: an *in-vitro*, *in-vivo* and *in-silico* approach.

Jawad Khan[1], Gowhar Ali[*1], Umer Rashid[2], Rasool Khan[3], Muhammad Saeed Jan[4], Rahim Ullah[1], Sajjad Ahmad[5], Sumra Wajid Abbasi[6], Atif Ali Khan Khalil[6], Robert D. E. Sewell[7]

[1]Department of Pharmacy, University of Peshawar, Peshawar 25120, Pakistan
[2]Department of Chemistry, COMSATS University Islamabad, Abbottabad Campus, Pakistan
[3]Institute of Chemical Sciences, University of Peshawar, Pakistan 25120, Pakistan
[4]Department of Pharmacy, Faculty of Biological Sciences, University of Malakand, Chakdara 18000 Dir (L), Pakistan
[5]Department of Health and Biological Sciences, Abasyn University, Peshawar 25000, Pakistan
[6]Department of Biological Sciences, National University of Medical Sciences, Rawalpindi, 46000, Pakistan
[7]School of Pharmacy and Pharmaceutical Sciences, Cardiff University, Cardiff CF10 3NB. UK

*** Corresponding author:**

Dr. Gowhar Ali,
(B.Sc., Pharm.D., Ph.D.)
Assistant Professor
Department of Pharmacy
University of Peshawar,
Peshawar-25120, KP, PAKISTAN.
Cell # 00923339317832
Contact: Tel: *+92 091 9216750;*
Fax:+92-91-9218131
ORCID:: https://orcid.org/0000-0002-9749-0645

Highlights

-A synthesised anti-inflammatory cyclohexanone (CHD) was tested *in vivo* and *in vitro*

-CHD inhibited COX-2 and 5-LOX enzymes plus COX-2, TNF-α and IL-1β mRNA expression

-CHD also produced $GABA_A$ and opioid mediated inhibitory activity in nociceptive tests

-In silico CHD had preferential affinity for $GABA_A$, opioid and COX-2 target sites

-CHD may possess therapeutic effectiveness in the management of inflammation and pain

Graphic Abstract

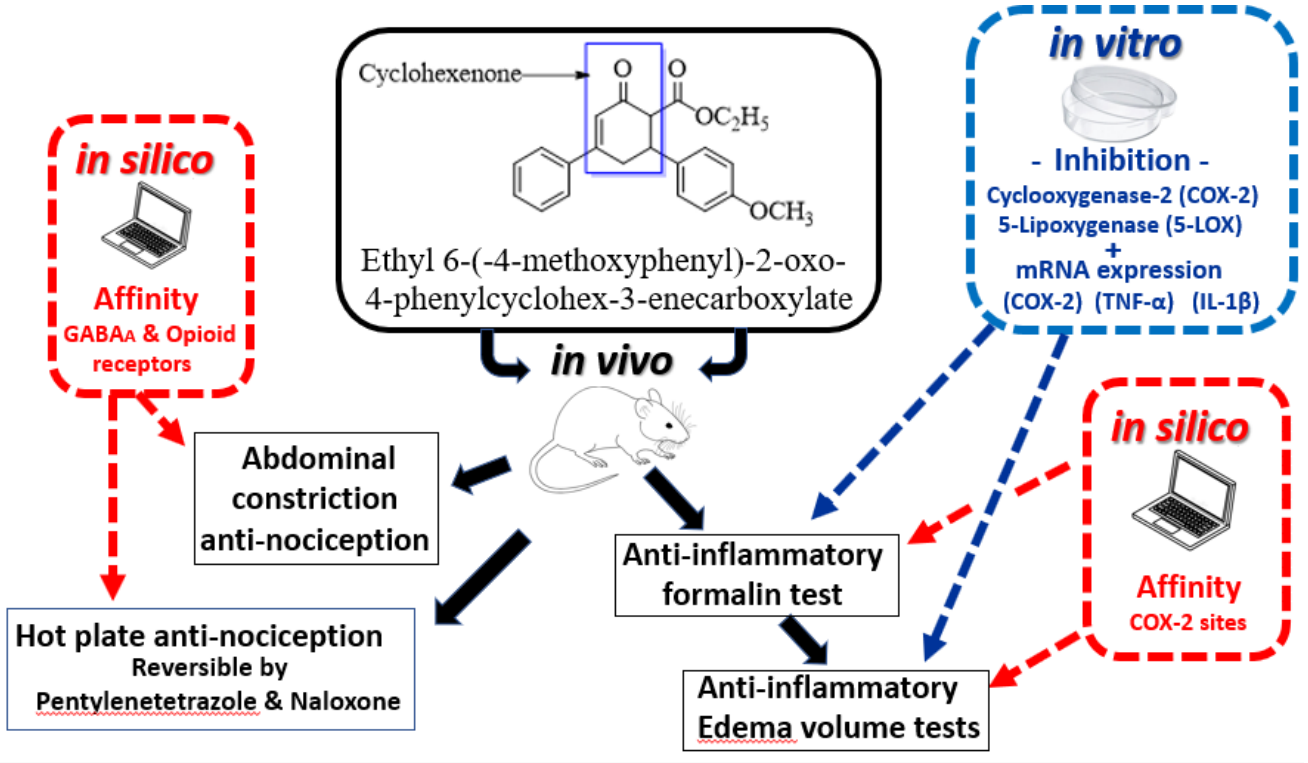

Abstract

The synthesis of a novel cyclohexanone derivative (CHD; Ethyl 6-(4-metohxyphenyl)-2-oxo-4-phenylcyclohexe-3-enecarboxylate) was described and the subsequent aim was to perform an *in vitro*, *in vivo* and *in silico* pharmacological evaluation as a putative anti-nociceptive and anti-inflammatory agent in mice. Initial *in vitro* studies revealed that CHD inhibited both cyclooxygenase-2 (COX-2) and 5-lipoxygenase (5-LOX) enzymes and it also reduced mRNA expression of COX-2 and the pro-inflammatory cytokines TNF-α and IL-1β. It was then shown that CHD dose dependently inhibited chemically induced tonic nociception in the abdominal constriction assay and also phasic thermal nociception (i.e. anti-nociception) in the hot plate and tail immersion tests in comparison with aspirin and tramadol respectively. The thermal test outcomes indicated a possible moderate centrally mediated anti-nociception which, in the case of the hot plate test, was pentylenetetrazole (PTZ) and naloxone reversible, implicating GABAergic and opioidergic mechanisms. CHD was also effective against both the neurogenic and inflammatory mediator phases induced in the formalin test and it also disclosed anti-inflammatory activity against the phlogistic agents, carrageenan, serotonin, histamine and xylene compared with standard drugs in edema volume tests. *In silico* studies indicated that CHD possessed preferential affinity for $GABA_A$, opioid and COX-2 target sites and this was supported by molecular dynamic simulations where computation of free energy of binding also favored the formation of stable complexes with these sites. These findings suggest that CHD has prospective anti-nociceptive and anti-inflammatory properties, probably mediated through GABAergic and opioidergic interactions supplemented by COX-2 and 5-LOX enzyme inhibition in addition to reducing pro-inflammatory cytokine expression. CHD may therefore possess potentially beneficial therapeutic effectiveness in the management of inflammation and pain.

Keywords

Cyclohexenone, Anti-nociceptive, Anti-inflammatory, Cyclooxygenase-2, 5-lipoxygenase, $GABA_A$/opioid receptors

1. Introduction

The process of drug discovery and development incorporating a novel chemical moiety with a desirable therapeutic profile is a challenging task nowadays (DiMasi et al., 2010). Extensive research has been carried out on pain and inflammation over a number of years, particularly because these pathological conditions can greatly influence patient quality of life (Ali et al., 2015; Chapman and Gavrin, 1999; Shahid et al., 2017a; Shahid et al., 2017b). Pathologically, pain may be categorized as nociceptive, neuropathic or inflammatory and if protracted, it may progress into a chronic pain syndrome involving additional symptoms such as anxiety and depression. Nociceptive pain is typically initiated by stimulation of somatic sensory receptors designated as nociceptors, which then transmit pain impulses to the central nervous system (CNS). Alternatively, neuropathic pain arises from damage or lesions to the nervous system (Van Hecke et al., 2014). Active inflammation is the hallmark of inflammatory pain and is characterized by the presence of inflammatory mediators such as interleukin, TNF-α, prostaglandins (PGE2, PGI2, TXA2), histamine, serotonin, bradykinin and leukotrienes (LTs) (Fernandes et al., 2015). These biochemical substances produce changes in neuronal sensitivity and invoke the onset of tissue hypersensitivity associated with inflammation (Kidd and Urban, 2001). Currently, opioids and non-steroidal anti-inflammatory drugs (NSAIDs) are the analgesic agents of choice often utilized in the management of inflammatory pain. However, it is well documented that persistent use of NSAIDs may well cause deleterious effects such as ulceration, hemorrhage or even perforation in the gastrointestinal tract, cardiovascular system disorders and kidney damage (Gutthann et al., 1996; Jones et al., 2008). Similarly, opioid analgesics are considered highly effective as analgesics, but they are associated with dependence liability and other side effects which may limit their

usefulness (Laxmaiah Manchikanti et al., 2010; Mayer et al., 1995; Shahid et al., 2016). Consequently, there is a genuine need for substitute drugs that retain the analgesic and anti-inflammatory effectiveness of conventional analgesic agents without their untoward effects (Fawad et al., 2018; Islam et al., 2017; Islam et al., 2019).

The key role of the cyclohexenone ring is well established in the field of biomedical research. It has been documented that this functionality is an integral part of several interesting compounds and is of considerable significance for the development of potentially valuable drugs (Das and Manna, 2015; Fang et al., 2012). Chemically, the cyclohexenone nucleus, serves as a convenient intermediate for synthesizing various heterocyclic compounds including fused pyrazoles, isoxazoles, quinazolines (Senguttuvan and Nagarajan, 2010) and 2H-indazole (Gopalakrishnan et al., 2008). Cyclohexenones are cyclohexane derivatives with a carbonyl group at position-1 and a carbon-carbon double bond at position-2 (Fig. 1). The enone functional group and substitution at a carbon atom in the six membered ring have been used to synthesize other substituted cyclohexenones (Johnson et al., 2016). The pharmacological properties of cyclohexenone derivatives include anti-inflammatory and anti-nociceptive effects (Ahmadi et al., 2012; Lednicer et al., 1981a; Lednicer et al., 1981b; Liu et al., 2013; Ming-Tatt et al., 2013; Ming-Tatt et al., 2012; Sheorey et al., 2016; Wang et al., 2011) as well as anti-neuropathic and antioxidant activity (Khan et al., 2019). The present study was undertaken to evaluate a novel cyclohexenone derivative (CHD; Ethyl 6-(4-metohxyphenyl)-2-oxo-4-phenylcyclohexe-3-enecarboxylate) as a possible inhibitor of cyclooxygenase-2 (COX-2) and 5-LOX pro-inflammatory enzymes and subsequently examine its effects against nociception using *in vivo* mouse models of pain and inflammation. Additionally, the anti-nociceptive activity of CHD was also investigated in the presence of

pentylenetetrazole (PTZ) and naloxone in order to probe any possible underlying mechanisms, which might have been corroborated by *in silico* and *in vitro* studies.

2. Material and methods

2.1. *Chemicals and drugs*

Naloxone, serotonin, histamine, PTZ, xylene, indomethacin, lambda carrageenan and aspirin were purchased from (Sigma-Aldrich, USA). Formaldehyde was procured from Merck (Germany), glacial acetic acid was obtained from Pancreac (Spain), tramadol (Tramal® 50mg/ml) was acquired from Searle Ltd (Pakistan). Fresh preparation of chalcone was carried out in the laboratory of ICS (University of Peshawar, Pakistan). Ethyl acetoacetate, ethyl acetate and potassium carbonate were purchased from Merck (Pakistan). N-hexane and ethanol were procured from Scharlau (Lahore, Pakistan). The cDNA synthesis kit, TRIzol reagent, master mix and primers were acquired from Thermofishcer Scientific (USA).

2.2. Chemistry

2.2.1. General

A Gallenkamp melting point apparatus was used to determine melting points. Purity was checked by thin layer chromatography (TLC). A Shimadzu IR Prestige-21 FT-IR Spectrometer Instrument (Tokyo, Japan) was utilized to record the Infrared spectra. ^{13}C and ^{1}H NMR analyses (Agilent AV-300,400 and 500 Tokyo, Japan) were accomplished with D_2O and DMSO-d_6 as solvents. Mass spectra (ESI-MS) were obtained on (Qp 2010 plus, Shimadzu, Tokyo, Japan). Perkin Elmer 2400 CHN/O Analyzer was operated to determine Elemental analysis.

148 *2.2.2. Synthesis of Ethyl 6-(4-metohxyphenyl)-2-oxo-4-phenylcyclohexe-3-enecarboxylate*

149 The synthesis was conducted according to the synthetic protocol as shown in Scheme 1. (E)-3-(-
150 4-methoxyphenyl)-1-phenylprop-2-en-1-one (10 mmol) was refluxed with ethyl acetoacetate (20
151 mmol) in the presence of K_2CO_3 catalyst in 20 ml of ethanol for 3 hr. The product obtained was
152 recrystallized from ethanol; a brownish yellow powder was obtained having a yield of 85 %. M.p
153 = 92-95 ^{0}C; Rf = 0.51 *n*-Hexane/ethyl acetate (7:3); IR (KBr) υmax cm-1: 3077 (Ar-H), 1689
154 (ketone C=O), 1735 (Ester C=O) 2870 (Aliphatic C-H); ^{1}H-NMR ($CDCl_3$, 400MHz) δ:6.9-7.5 (m,
155 Ar-H),3.05 (d, 2H, J= 2.3), 2.9 (t,1H J=5.0, C-3), 2.6-2.8(q, 5H, CH_2CH_3, J=7.0); ^{13}C-NMR (100
156 MHz, $CDCl_3$) δ: 199.0 (C=O), 125-130 (Ar-CH), 112 (C-6), 40.2 (OCH_3), 159.0 (C-19), and 44.39
157 (C-3). EI-MS; m/z (rel. int. %) 351 (M+), CHN Anal. Calcd for: C, 75.41; H, 6.33; O, 18.26.
158 Found: C, 74.81; H, 6.38. Formula: $C_{22}H_{22}O_4$, C=22, H=22, and O=4.

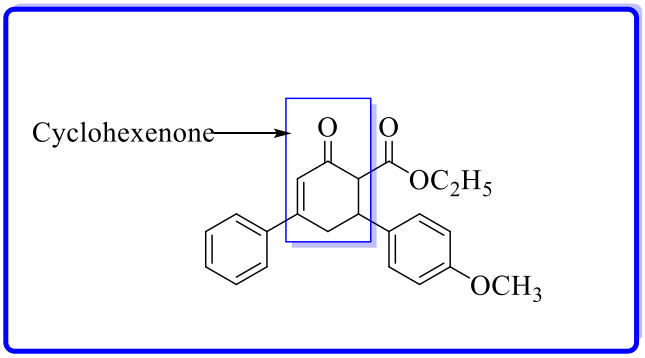

159

160 **Fig. 1.** Chemical structure of Ethyl 6-(-4-methoxyphenyl)-2-oxo-4-phenylcyclohex-3-
161 enecarboxylate

162

163

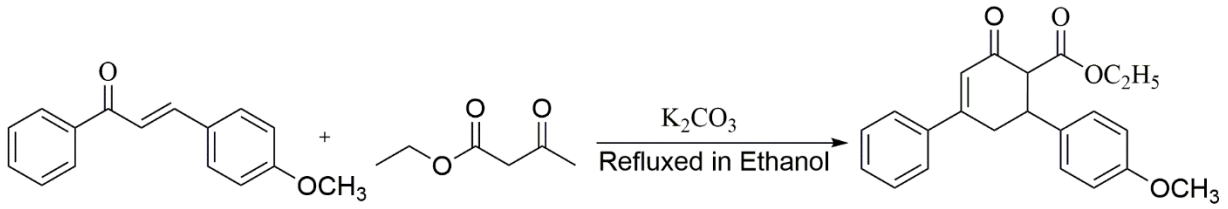

Scheme 1. Synthetic scheme of Ethyl 6-(4-metohxyphenyl)-2-oxo-4-phenylcyclohexe-3-enecarboxylate

2.3. In vitro activities

2.3.1. 5-LOX inhibition assay

The inhibitory potential of CHD was examined by utilizing human recombinant 5-LOX. In this assessment, the enzyme inhibition was determined through residual enzyme potential following 10 to 15 min incubation at 25 ^{o}C in an incubator (Jan et al., 2020; Wisastra et al., 2013). The activity was estimated through linoleic acid (lipoxygenase substrate) conversion into hydroperoxy-octadecadienoate (HPOD). The alteration rate was calculated in the form of absorbance at 234 nm with UV- visible spectrophotometer. Ethylene diamine tetra acetic acid (EDTA 2 mM) and $CaCl_2$ (2 mM) containing Tris buffer (50 mM) of PH 7.5 was used as an assay buffer for this assay. The enzyme 5-LOX (20,000 U/ml) was diluted with buffer in a ratio of 1:4000. The assay buffer was then diluted with 100 mM of inhibitor formerly blended with DMSO. Linoleic acid was then diluted with ethyl alcohol to 20 mM. Subsequently, various concentrations of CHD ranging from 31.25 to 1000 µg/ml and 1 ml of enzyme solution (1:4000) was mixed with 100 µl adenosine triphosphate (2 mM), 790 µl of Tris buffer plus 100 µl inhibitor (1mM) and then incubated for ten min duration. Then to this mixture was added 10 µl of substrate solution (20mM) and after ten seconds mixing of the enzyme with substrate, the substrate conversion rate was monitored. The

reaction rate in the absence of inhibitor was employed as positive control. The standard inhibitor agent used in this assay was zileuton.

2.3.2. COX-2 Inhibition assay

The COX-2 inhibitory activity of the test compound was evaluated according to a previously validated procedure (Burnett et al., 2007; Jan et al., 2020). A COX-2 enzyme solution (300 U/ml) was prepared. For activation, 10 µl of enzyme solution was kept for 5 to 6 min on ice (4 ^{o}C) and then mixed with 50 µl of co-factor solution comprising 0.9 mM glutathione, 1 mM hematin in 0.1 mM Tris buffer (pH 8.0) and 0.24 mM tetramethyl-p-phenylenediaminedihydrochloride (TMPD). Then various concentrations (31.25 to 1000 µg/ml) of test sample (20 µl) plus enzyme solution (60 µl) were maintained at room temperature for 5 to 10 min, followed by initiation of the reaction by adding 30 mM arachidonic acid (20 µl) and keeping this mixture at 37 ^{o}C for a duration of 15 min. Afterwards, the reaction was terminated by addition of hydrochloric acid (HCL) and absorbance was measured via a UV-visible spectrophotometer at 570 nm. COX-2 percentage inhibition was calculated from the absorbance value per unit time. In the study Celecoxib was utilized as the standard inhibitor agent.

2.3.3. Reverse transcription polymerase chain reaction (RT-PCR)

Post-mortem mouse paw sub plantar tissues were removed 5 h after carrageenan administration and RNA was extracted using TRIzol reagent according to the manufacturer's protocol. The total RNA was reverse transcribed to cDNA following a standard protocol. The primers for targeted genes use were;

COX-2: F-5'-GGAGAGACTATCAAGATAGTGATC -3', R- 5'- ATGGTCAGTAGA-CTTT-TACAGCTC-3'. **TNF-α:** F-5'-CTTCTCCTTCCTGATCGTGG-3'; R-5'-GCTGGTTAT-

CTCTCAGCTCCA-3'. **IL-1β**: F-5'-AGAAGCTTCCACCAATACTC-3', R-5'-AGCACCTAG-TTGTAAGGAAG-3'. **GAPDH**: F-5'-TGCACCACCAACTGCTTAGC-3'; R- 5'-GGCATG-GACTGTGGTCATGAG3' was used as a housekeeping gene (Cheon et al., 2009; Khalid et al., 2018). Amplified products were separated using 1.5% Agarose gel electrophoresis, analyzed with image J software (Almeer et al., 2019; Ullah et al., 2021).

2.4. In vivo pharmacological evaluation

2.4.1. Animals

Mice (Balb-C) of either sex weighing 18-30 g were used during the investigation unless otherwise stated. Animals were maintained on standard laboratory food and water *ad libitum* at an ambient temperature of 22 ± 2^{o}C through a thermostatically controlled air conditioning system on a 12/12 h light and dark cycle and they were habituated to laboratory conditions for two h before experiments.

2.4.2. Ethical approval

The study and all *in vivo* protocols were conducted under a project entitled "Studies on the nociceptive, inflammatory and neuropathic pain relieving potential of a cyclohexenone derivative." It was approved by the Research Ethical Committee of the Department of Pharmacy, University of Peshawar, Pakistan which issued a certificate number of 01/EC/18/Pharm. Furthermore, animal experiments were performed in compliance with the Animals Scientific Procedure Act UK (1986).

228 *2.4.3. Acute toxicity study of compound CHD*

229 The acute toxicity profile of CHD was evaluated after intraperitoneal (i.p) injection of selected
230 doses (on a sequential dose-doubling increasing scale viz 15, 30, 60, 120 or 240 mg/kg (n=6)).
231 Animals were observed at 30-60 min and 24-72 h for any abnormal behaviour (Akbar et al., 2016).

232 *2.4.4. Anti-nociceptive activity*

233 *2.4.4.1. Anti-nociceptive activity of compound CHD and a standard drug in the acetic acid*
234 *abdominal constriction test*

235 Food and water were withdrawn 120 min prior to animal experiments. One percent acetic acid (10
236 ml/kg) i.p injection was used to induce abdominal constriction as a reflection of tonic nociception.
237 Five min after acetic acid i.p injection, the incidence of abdominal constrictions was recorded over
238 a 20 min period (Abbas et al., 2011). The animals were randomly allocated to different
239 investigational groups (n=6). Group I received normal saline as vehicle, group II-IV received
240 standard aspirin (15-45 mg/kg), group V-VII received test compound (CHD) (15-45 mg/kg) via
241 i.p injection, 30 min prior to 1% acetic acid injection. Percentage analgesia was calculated using
242 the following formula:

243 % protection = (1- mean number of abdominal constrictions of the treated drug / mean number
244 of abdominal constrictions of the vehicle control) × 100

245 *2.4.4.2. Anti-nociceptive activity of compound CHD compared to a standard drug in the hot plate*
246 *test*

247 The hot plate analgesiometer, was kept at a constant temperature of 54 ± 0.1^{0} C. After placement on
248 the plate, animal nociceptive reaction latencies (s) were determined to the following escape end
249 points: paw licking, flinching or jumping and a 30 s cut off time was imposed after which mice

were removed from the stimulus (Ahmad et al., 2017; Rukh et al., 2020). Animals were randomly assigned to groups (n=6) and administered saline or drug treatment intraperitoneally. Group I received normal saline as vehicle, group II received standard drug (tramadol, 30 mg/kg, i.p), groups III-V received the trial compound (CHD, 15-45 mg/kg, i.p).

2.4.4.3. Pharmacological antagonism study of CHD compared to a standard drug

In order to evaluate the possible involvement of $GABA_A$ or opioid receptors in the anti-nociceptive activity of CHD, mice were administered PTZ (15 mg/kg; i.p) or naloxone (1 mg/kg; subcutaneously (s.c)) 10-20 min prior to i.p dosing with saline, CHD or standard drug. Hot plate latencies were recorded 30,60 and 90 min after administration of each drug (Muhammad et al., 2012). Percentage protection against nociception was determined using the following formula:

% protection = (Test latency−baseline latency)/ (cut off time−baseline latency) × 100

2.4.4.4. Anti-nociceptive activity of CHD compared to a standard drug in the tail immersion test

Each animal was gently held in a vertical position and half of the tail was immersed in a water bath maintained at a temperature of 55±0.5 ^{o}C. A nociceptive reaction latency (s) was determined to a tail flick end point and a cut off time of 15 s imposed after which animals were removed from the stimulus. Any non-responders within the cut-off time were excluded from the study. The vehicle, standard tramadol (30 mg/kg) and test compound (15-45 mg/kg) were administered i.p to their respective groups. The readings were taken at 30, 60, 90 and 120 min after drug administration (Sewell and Spencer, 1976).

2.4.4.5. Anti-nociceptive activity of CHD and standard drug in the formalin induced biphasic pain model

Mice were administered a sub plantar injection of 20µl of freshly prepared 2 % formalin in the right hind paw. Thirty min prior to formalin injection, groups I-VI, received intraperitoneally normal saline as vehicle, standard drugs indomethacin (10 mg/kg) or diclofenac (10 mg/kg), and CHD (15-45mg/kg). The nociceptive reaction time (s) (latency to biting, licking, paw lifting or flinching) was measured in two phases: first phase (0 to 5 min) and second phase (10-30 min) after the formalin injection (Silva et al., 2017; Maione et al., 2020).

2.4.5. Anti-inflammatory activity

2.4.5.1. Anti-inflammatory activity of compound CHD and standard in a carrageenan induced paw edema model

Mice were treated with normal saline, aspirin (50-150 mg/kg) or test compound (CHD, 15-45 mg/kg, i.p) 30 min before s.c injection of 0.05 ml of freshly constituted carrageenan (1 %) in the right hind paw. A digital Plethysmometer was utilized to determine the inflammation in terms of paw edema volume (ml) at hourly intervals up to 5 h post carrageenan injection (Ali et al., 2013).

2.4.5.2. Anti-inflammatory activity of compound CHD and standard drug in a histamine induced paw edema model

Inflammation was induced in mice (25-30 g) by sub plantar injection of 0.1 ml freshly constituted histamine (1 mg/ml) in the right hind paw. Paw inflammation swelling was measured by means of plethysmometer previously described in the carrageenan test (Mequanint et al., 2011).

292 *2.4.5.3. Anti-edema activity of CHD and a standard drug in the serotonin induced paw volume*
293 *model*

294 Mice were administered serotonin (0.001 mg/ml s.c) into the plantar surface of the right hind paw.
295 The ensuing inflammation and paw edema was measured by plethysmometer (Masresha et al.,
296 2012).

297 *2.4.5.4. Anti-inflammatory action of compound CHD and standard drug in the xylene provoked*
298 *ear edema model*

299 In mice weighing 25-35 g, ear edema was evoked by topical application of 0.03 ml of xylene to
300 the internal and outer surface of the right ear while the left ear was used as control. Thirty min
301 before induction of xylene edema, saline vehicle was administered i.p to group I, standard
302 indomethacin (10 mg/kg) or diclofenac (15 mg/kg) to groups II-III and test compound CHD (15-
303 45 mg/kg) to groups IV-VI respectively. Subsequently, 15 min after xylene application, animals
304 were killed and the ears were amputated then weighed. The mean weight difference between right
305 and left ears was then determined (Manouze et al., 2017).

306

307

308

309 *2.5. In silico activity*

310 *2.5.1. Docking studies*

311 Docking studies were executed through the Molecular Operating Environment (MOE) version
312 2016.08 docking program. Three-dimensional (3D) structures of the enzymes, $GABA_A$ and opioid
313 receptors with their co-crystalized ligands were obtained from the Protein Data Bank as listed in

Table 1. The docking algorithm was validated by re-docking of native ligands as shown in Table 1. The computed root mean square deviation (RMSD) between the experimental and re-docked poses was found within a threshold limit < 2 Å. The 3D structures of the compound were constructed in MOE by utilizing Builder Module. Energy minimization of the ligand, preparation of structures of the downloaded enzymes and active site identification was carried out according to our earlier validated methods (Iftikhar et al., 2017; Iftikhar et al., 2018; Rashid et al., 2016). Assessment of docking outcomes and scrutiny of their surface with graphical demonstrations were accomplished with discovery studio visualizer and MOE (Systemes, 2015).

Table 1

Protein Data Bank (PDB) code numbers, names of their co-crystalized ligands and resolution for the enzymes studied.

Enzyme/Receptor	PDB code	Co-crystalized ligand	Resolution (Å)
COX-1 enzyme	1EQG	Ibuprofen	2.61
COX-2 enzyme	1CX2	1-Phenylsulfonamide-3-trifluoromethyl-5-parabromophenylpyrazole (SC-558)	3.00
$GABA_A$ receptor	4COF	Benzamidine	2.97
μ-opioid receptor	4DKL	β-Funaltrexamine (μ-opioid receptor antagonist)	2.8
δ-opioid receptor	4EJ4	Naltrindole (δ-opioid receptor antagonist)	3.4
κ-opioid receptor	4DJH	(3R)-7-Hydroxy-N-{(2S)-1-[(3R,4R)-4-(3-hydroxyphenyl)-3,4-dimethylpiperidin-1-yl]-3-methylbutan-2-yc-1,2,3,4-tetrahydroisoquinoline-3-carboxamide (JDC)	2.9

330 *2.5.2. Molecular Dynamic Simulation of Complexes*

331 Molecular Dynamic (MD) simulations were performed using the same protocol as explained in
332 our previous study (Abbasi et al., 2016). MD simulations facilitate understanding of the binding
333 pattern and determine the stability of selected receptor-CHD docked complexes. Using AMBER
334 18 software, six different systems were prepared to run MD simulations for 50 ns each (Case et
335 al., 2010). In order to verify the structural variations and convergence of the simulated systems,
336 the CPPTRAJ module of AmberTools18‘s was used to estimate the RMSDs for all the studied
337 systems.

338 *2.5.2.1. Binding Free Energy Calculations*

339 The MMPB/GBSA methods, integrated in AMBER 18, were employed to calculate the binding
340 free energies for all six systems (Miller III et al., 2012). Binding free energy calculations were
341 performed on 100 snapshots taken from the MD trajectories as described previously by Abro and
342 Azam (Abro and Azam, 2016). The binding free energy can be expressed as:
343 $\Delta G_{bind} = \Delta G_{complex} - [\ \Delta G_{receptor} + \Delta G_{ligand}]$
344 where ΔG is the Gibb's free energy calculated by MMGB/PBSA.

345 *2.6. Statistical analysis*

346 The data were analyzed statistically utilizing Graph Pad Prism Software, version 5, for manifold
347 assessments via one-way analysis of variance (ANOVA) with Post-hoc Dunnett’s test. Outcomes
348 were regarded as statistically significant at $P < 0.05$.

349 **3. Results**

350 *3.1. In vitro activities*

351 All enzyme suppression results are presented as the mean of triplicate determinations for each
352 concentration studied and an IC_{50} value was extrapolated from the overall inhibitory concentration
353 relationships.

354

355

356 *3.1.1. 5-LOX inhibitory activity*

357 The 5-LOX inhibitory activity of CHD was examined at various concentrations ranging from 31.25
358 to 1000 µg/ml and the compound displayed a potent inhibition of 5-LOX with an extrapolated IC_{50}
359 value of 10. 27 µg/ml as compared to the standard 5-LOX inhibitor drug zileuton (extrapolated
360 IC_{50} = 5.50 µg/ml) over the same tested concentration range (Table 2).

361 *3.1.2. COX-2 inhibitory activity*

362 CHD disclosed a potent inhibitory action on the COX-2 enzyme as shown in Table 3. It was also
363 evident from the outcomes that CHD possessed valuable COX-2 inhibitory activity in comparison
364 with the standard COX-2 inhibitor drug celecoxib. Thus, the IC_{50} value for CHD was extrapolated
365 as 8.94 µg/ml in contrast to that of celecoxib (IC_{50} = 4.30 µg/ml) (Table 3).

366 **Table 2**

367 5-LOX enzyme inhibitory activity of CHD in comparison with zileuton as a standard 5-LOX
368 inhibitor drug.

Compound	**Conc. (µg/ml)**	**% 5-LOX inhibition (Mean ± S.E.M)**	**Extrapolated IC_{50} µg/ml**
Cyclohexenone derivative (CHD)	1000	89.44 ± 0.55[b]	10.27
	500	83.17 ± 0.72[c]	
	250	78.30 ± 0.64[c]	
	125	73.34 ± 0.63[c]	
	62.5	68.30 ± 0.64[c]	
	31.25	61.93 ± 1.13[c]	
Zileuton	1000	93.55 ± 0.40	5.50
	500	89.37 ± 1.65	
	250	85.50 ± 0.40	
	125	79.60 ± 0.90	
	62.5	74.17 ± 0.72	
	31.25	70.35 ± 0.45	

369 Data is represented as mean ± S.E.M; Values were significantly different ~~as~~ compared to the
370 positive control (zileuton); n=3, b= $P < 0.01$, c=$P < 0.001$.

Table 3

COX-2 enzyme inhibitory assay of CHD in comparison with celecoxib as a standard COX-2 inhibitor drug.

Compound	Conc. (µg/ml)	% COX-2 inhibition (Mean ± S.E.M)	Extrapolated IC_{50} µg/ml
Cyclohexenone derivative (CHD)	1000	88.91 ± 1.30[c]	8.94
	500	85.00 ± 0.30[c]	
	250	78.76 ± 0.58[c]	
	125	73.67 ± 0.61[c]	
	62.5	67.74 ± 0.61[c]	
	31.25	63.47 ± 0.56[c]	
Celecoxib	1000	95.20 ± 0.15	4.30
	500	91.17 ± 0.53	
	250	86.98 ± 0.85	
	125	81.20 ± 0.65	
	62.5	77.80 ± 0.37	
	31.25	73.11 ± 1.20	

Data is represented as mean ± S.E.M; Values were significantly different ~~as~~ compared to the positive control (celecoxib); n=3, c=$P < 0.001$.

3.1.3. RT- PCR

To further investigate the anti-inflammatory potential of CHD, RT-PCR was utilized to assess the mRNA levels of COX-2 enzyme and the pro-inflammatory cytokines TNF-α and IL-1β in the carrageenan induced paw edema test in mice. The outcomes of this assessment revealed that CHD (45 mg/kg) significantly reduced the mRNA expression of COX-2 (P<0.001), while in the case of TNF-α and IL-1β, CHD also produced a reduction (P<0.01) compared to the carrageenan treated vehicle group. Aspirin (150 mg/kg) as the standard positive control decreased (P<0.001) the expression of COX-2, TNF-α and IL-1β as presented in (Fig. 2).

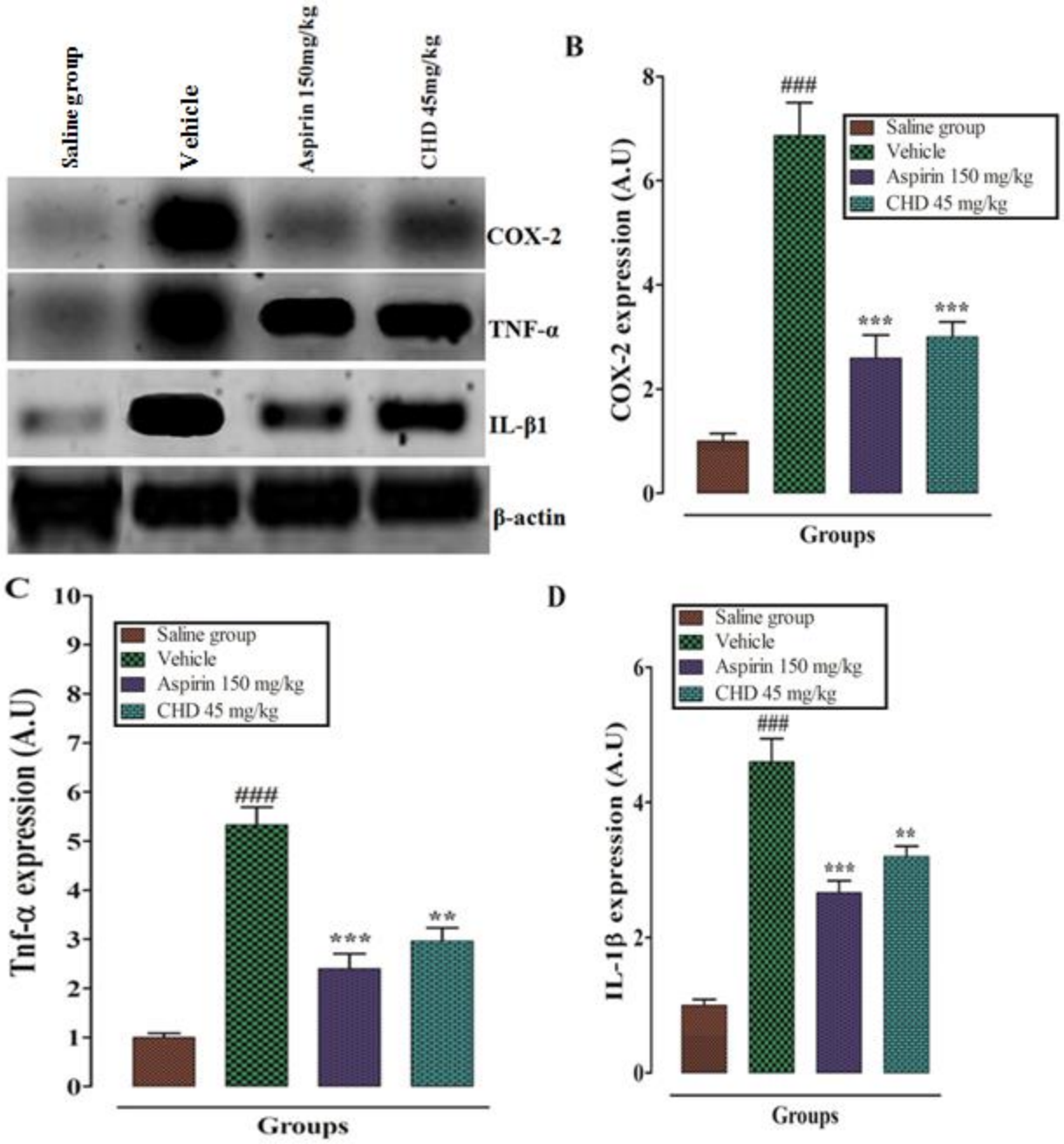

386

387 **Fig. 2.** Agarose gel electrophoresis (A) quantification of CHD activity on the mRNA level of
388 COX-2 **(B)**, TNF-α **(C),** and IL-1β **(D)** in carrageenan induced hind paw edema in mice. The results
389 are shown in relative arbitrary units (A.U). Bars represent mean expression in A.U ± S.E.M. ###
390 $P < 0.001$ compared to the saline group. $^{**}P < 0.01$, $^{***}P < 0.001$ compared to the vehicle group.

391

392

393 *3.2. In vivo pharmacological activity*

394 *3.2.1. Acute toxicity of CHD*

395 After i.p. injection of selected doses of CHD (15-240 mg/kg; $n = 6$), there was no acute toxicity
396 observed in gross animal behaviour, neither was any incidence of mortality recorded up to the
397 highest dose. Thus, the maximum tolerated dose (MTD) which was devoid of unacceptable toxicity
398 for CHD was >240 mg/kg.

399 *3.2.2. CHD attenuation of chemically induced tonic nociceptive behaviour*

400 Injection of acetic acid (1%) was accompanied by a significant rise in the nociceptive response
401 perceived as an onset increase in the incidence of abdominal constriction. The percentage
402 protection against this chemically induced tonic nociception in the group of animals treated with
403 CHD at a lower dose (15 mg/kg) decreased the nociceptive response as evidenced by an increase
404 in the percentage protection (44.66%, $P < 0.05$). Likewise, the mid-range CHD dose (30 mg/kg)
405 also protected against acetic acid evoked abdominal constriction (49.78%, $P< 0.01$). and the higher
406 dose (45 mg/kg) had an even greater anti-nociceptive effect (59.81%) reflecting dose dependent
407 activity relative to the saline treated animals. The aspirin positive control also yielded a dose
408 dependant anti-nociceptive response (15-45 mg/kg) versus the saline controls (Fig. 3).

409

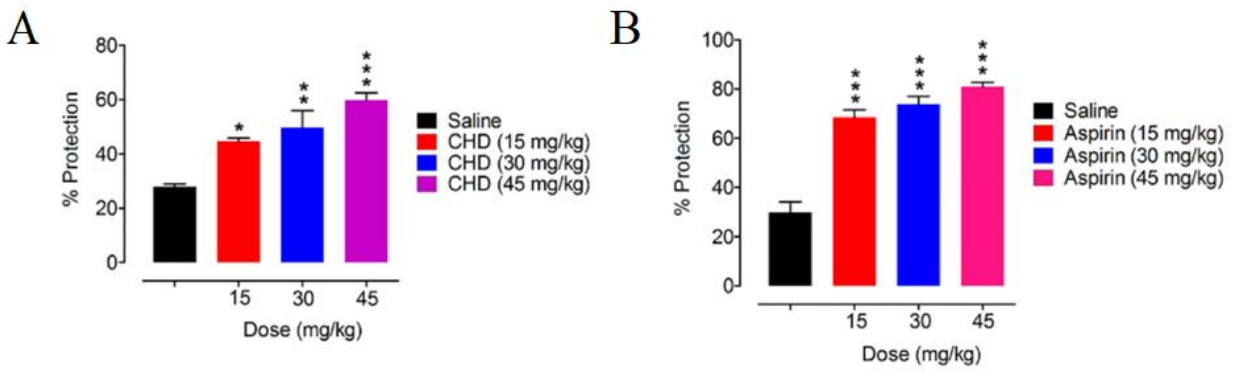

410

411 **Fig. 3.** Anti-nociceptive activity of (A) CHD and (B) the positive control, aspirin in the acetic acid
412 (1%) induced abdominal constriction test. Each bar represents mean percentage protection ±
413 S.E.M). **P*< 0.05, ***P*< 0.01, ****P*< 0.001 as compared to the saline treated group (one-way
414 ANOVA followed by *post hoc* Dunnett's test), (*n* = 6 mice per group).

415 *3.2.3. CHD attenuation of phasic thermal nociception*

416 In the hot plate test, the saline treated animal group displayed a control escape response from the
417 thermal nociceptive stimulus of 7.3%, 7.5% and 7.7% after 30, 60 and 90 min respectively. The
418 lower dose of CHD was ineffective in producing any detectable anti-nociception between 30-90
419 min (19.3%-17.6%). However, CHD at 30 mg/kg did produce an anti-nociceptive effect at 30 min
420 (24.5%) and 60 min (20.8%) but this was not evident after 90 min (19.5%). A greater anti-
421 nociceptive response was noted at the 45 mg/kg dose (27.3%, 24.0% and 20.3% at 30, 60 and 90
422 min respectively) while the tramadol (30 mg/kg) positive control produced an even bigger response
423 77.6%, 72.0% and 69.7% at 30, 60 and 90 min respectively (Fig. 4).

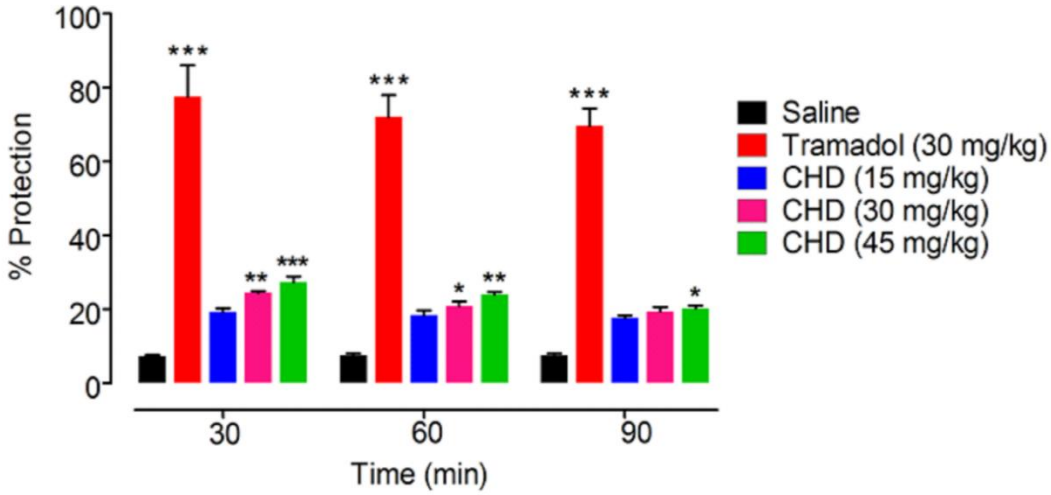

Fig. 4. Anti-nociceptive activity of CHD and the positive control, tramadol, in the hot-plate test. Each bar represents mean percentage protection ± S.E.M). **P*< 0.05, ***P*< 0.01, ****P*< 0.001 as compared to saline treated group (one-way ANOVA followed by *post hoc* Dunnett's test), (*n* = 6 mice per group).

3.2.4. CHD attenuation of phasic nociception in the tail immersion test

CHD produced a measurable anti-nociceptive response in the tail immersion test at the 30 mg/kg dose (30 min). However, the 45 mg/kg dose produced a peak response at 60 min which subsided by 120 min. Treatment with the positive tramadol control (30 mg/kg), produced an intense long-acting anti-nociceptive effect which lasted up to 120 min (Fig. 5).

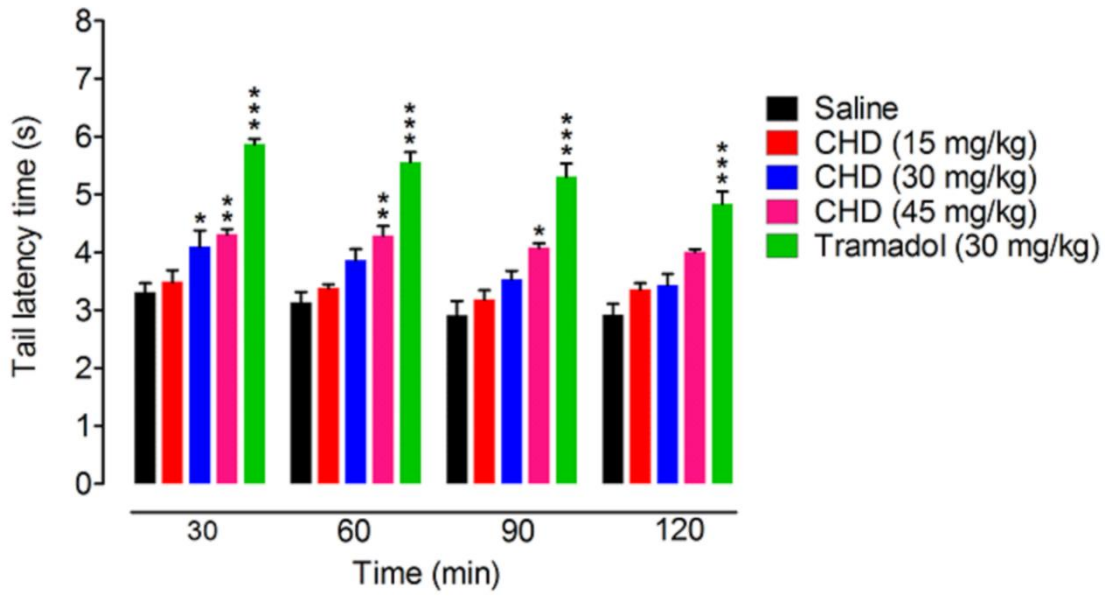

Fig. 5. Anti-nociceptive activity of CHD and the positive control, tramadol in the thermal tail immersion test. Each bar represents mean withdrawal latency time in s ± S.E.M). **P*< 0.05, ***P*< 0.01, ****P*< 0.001 as compared to saline treated group (one-way ANOVA followed by *post hoc* Dunnett's test), (*n* = 6 mice per group).

3.2.5. CHD attenuation of the formalin induced biphasic nociceptive response

Administration of formalin in the sub-plantar mouse hind paw initiated a marked nociceptive response as indicated by an increase in the duration of biting, licking, lifting and flinching of the affected paw. This was observed throughout the first phase (0-5 min) and also the second phase (15-30 min) following formalin administration in the saline treated animals. Treatment with CHD (15 mg/kg) only diminished the second phase of formalin induced nociception. Conversely, the 30 mg/kg CHD dose was more effective in that it markedly reduced the formalin nocifensive response in both the second and first phases (*P*< 0.05). Similarly, treatment with the higher CHD dose (45 mg/kg) did induce an anti-nociceptive response in the first phase, but a more statistically

448 significant response in the second phase. The indomethacin and diclofenac positive controls both
449 at 10 mg/kg generated comparable anti-nociception to CHD in both phases (Fig. 6).

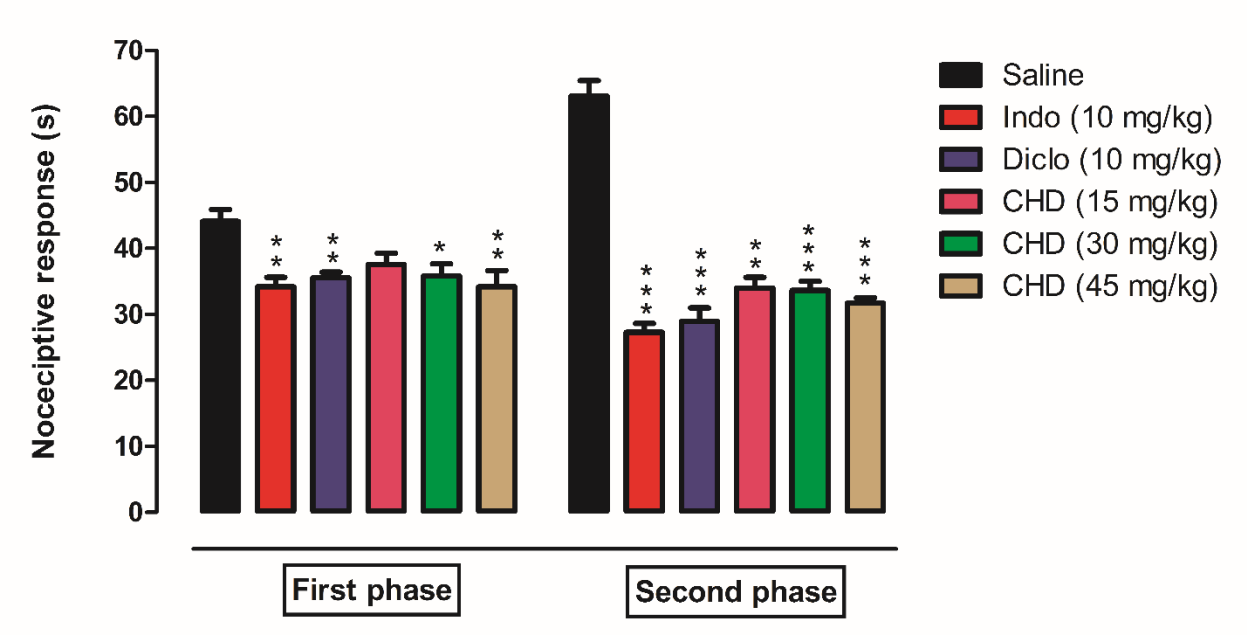

450

451 **Fig. 6.** Anti-nociceptive activity of CHD and the positive controls, indomethacin (Indo), and
452 diclofenac (Diclo) in the formalin induced paw nociceptive test. Each bar represents mean
453 nociceptive response in s ± S.E.M). **P*< 0.05, ***P*< 0.01, ****P*< 0.001 as compared to the saline
454 treated group (one-way ANOVA followed by *post hoc* Dunnett's test), (*n* = 6 mice per group).

455 *3.2.6. Opioidergic and GABAergic mediation of CHD anti-nociception*

456 Any possibility of GABAergic or opioidergic mechanisms underlying the anti-nociceptive effect
457 of CHD in the hot-plate test were probed using pentylenetetrazole (PTZ) and naloxone as
458 respective antagonists. Hence, the anti-nociceptive effect of CHD (30 and 40 mg/kg), was
459 significantly antagonized (*P*< 0.001) by naloxone (1 mg/kg) implicating the involvement of an
460 opioidergic mechanism. Likewise, in animals treated with the opioid agonist, tramadol (30 mg/kg)
461 as a positive control, naloxone also blocked the anti-nociceptive response (Fig. 7A).
462 Administration of PTZ (15 mg/kg) did not modify the ani-nociceptive action of tramadol (30

mg/kg), but it did markedly decrease the anti-nociceptive response of CHD (30 and 45 mg/kg) in the hot plate paradigm. This would tend to suggest an involvement of a GABAergic mechanism in the anti-nociceptive action of CHD but not tramadol (Fig. 7B).

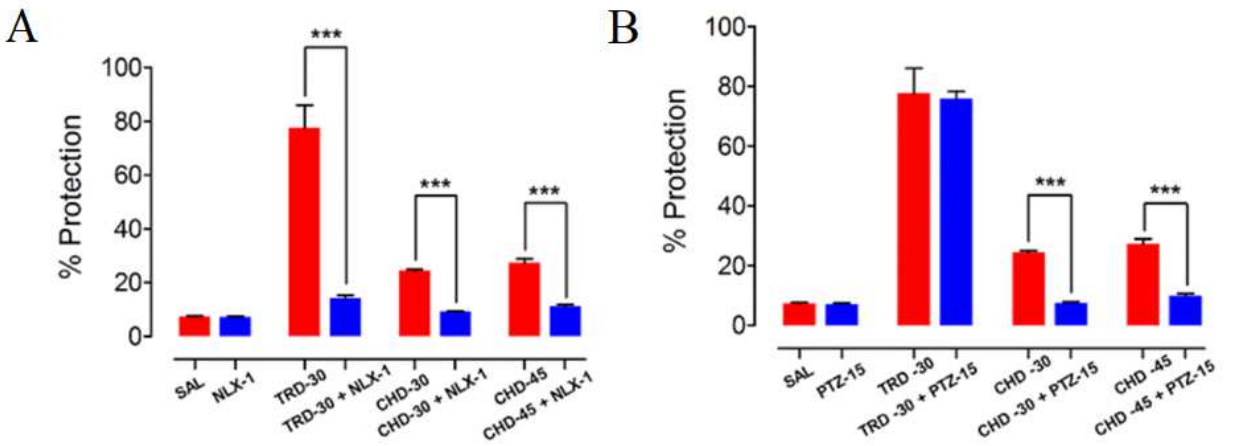

Fig. 7. (A) Effect of naloxone at 1 mg/kg (NLX-1) and (B) PTZ at 15 mg/kg (PTZ-15) on the anti-nociceptive activity of CHD (30 mg/kg, CHD-30 and 45 mg/kg, CHD-45) or tramadol (30 mg/kg, TRD-30) in the mouse hot-plate test. Each bar represents mean percentage protection ± S.E.M. ***$P < 0.001$ compared to saline control (SAL). (two sample *t*-test), ($n = 6$ mice per group).

3.2.7. Anti-inflammatory action of CHD against phlogistic agents (carrageenan, histamine, and serotonin) in the paw volume inflammation and xylene in the ear inflammation test

Intraplantar administration of the phlogistic agents, carrageenan, histamine, and serotonin was associated with a pronounced inflammatory response manifested by a substantial increase in the paw volume. The increased edema formation followed a temporal pattern and was first expressed during the initial h of the paradigm and maintained throughout the advanced stages of inflammation i.e. up to 5 h of the study duration. A dose dependent anti-inflammatory effect was produced by CHD in the three paradigms of paw edema. Treatment with CHD (15, 30 and 45 mg/kg) reduced the inflammatory response evoked up to 5 h after administration of carrageenan (Fig. 8A), histamine (Fig. 9A), and serotonin (Fig. 10A), Treatment with the aspirin positive

control, (50-150 mg/kg) consistently displayed an anti-inflammatory effect up to 5 h after injection of carrageenan, serotonin or histamine in the inflammatory paradigms (Figs 8B, 9B and 10B).

In the xylene provoked ear inflammatory edema paradigm, application of xylene produced a marked inflammatory response as observed by the increased ear weight recorded in the saline treated control animals (Fig 11). This marked oedematous change was significantly countered by treatment with CHD (30 and 45 mg/kg). The positive anti-inflammatory control drugs, indomethacin (10 mg/kg) and diclofenac (15 mg/kg) both produced a noteworthy decline in the augmented ear weight edema induced by xylene, as compared to the saline treated controls (Fig. 11).

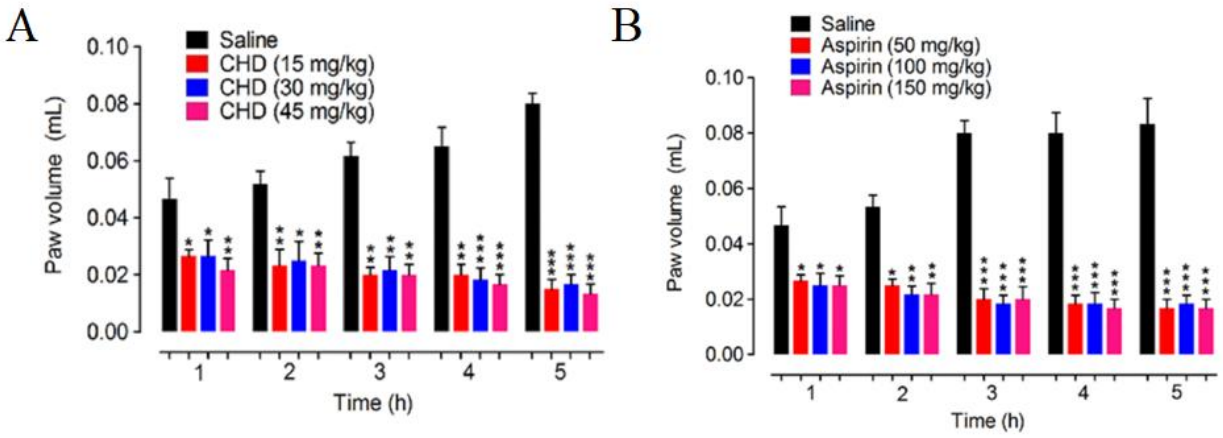

Fig. 8. Anti-inflammatory activity of (A) CHD and (B) the positive control, aspirin in the carrageenan induced paw edema test. Each bar represents paw volume in ml ± S.E.M. **P*< 0.05, ***P*< 0.01, ****P*< 0.001 as compared to saline treated group (one-way ANOVA followed by *post hoc* Dunnett's test), (*n* = 6 mice per group).

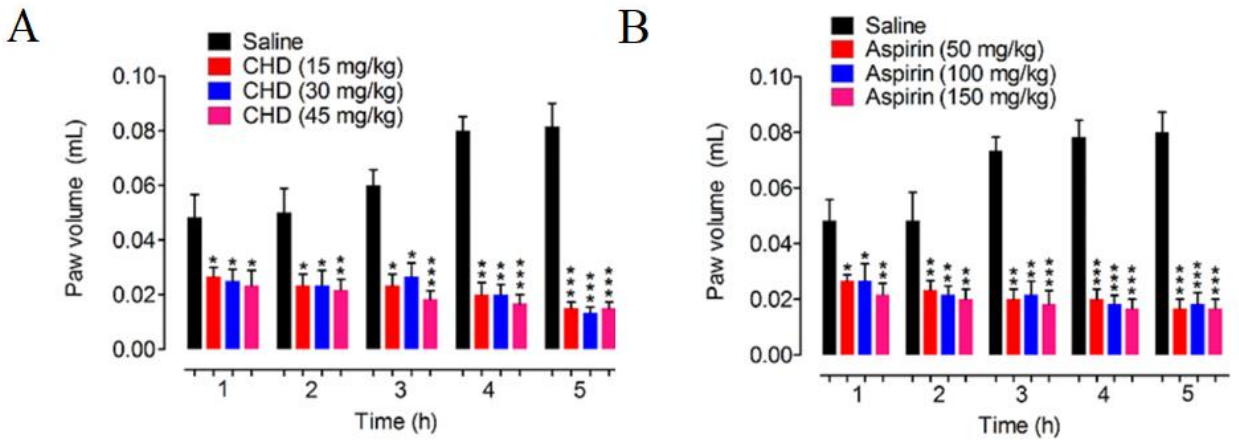

Fig. 9. Anti-inflammatory activity of (A) CHD and (B) the positive control, aspirin in the histamine induced paw edema test. Each bar represents paw volume in ml ± S.E.M. **P*< 0.05, ***P*< 0.01, ****P*< 0.001 as compared to saline treated group (one-way ANOVA followed by *post hoc* Dunnett's test), (*n* = 6 mice per group).

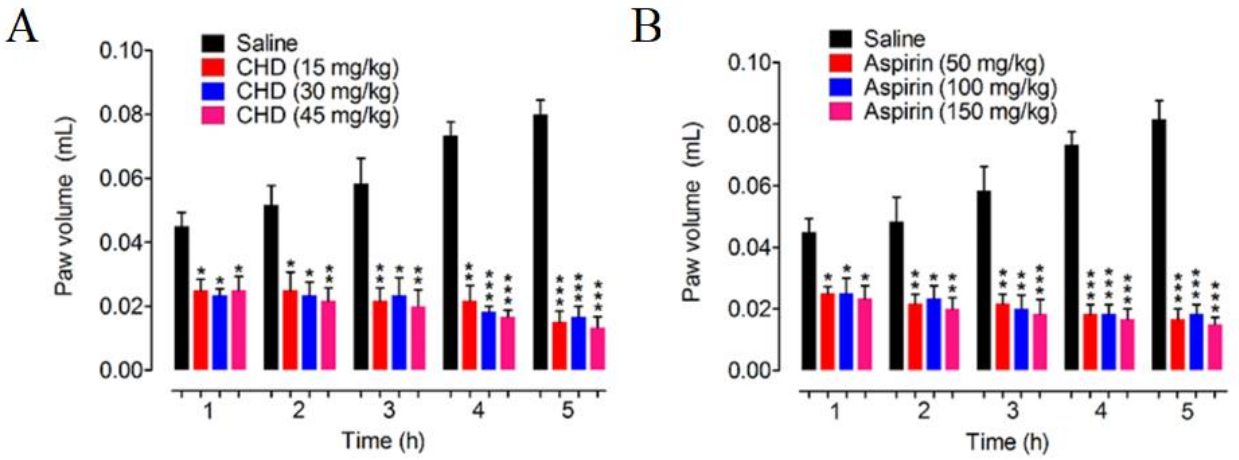

Fig. 10. Anti-inflammatory activity of (A) CHD and (B) the positive control, aspirin in the serotonin induced paw edema test. Each bar represents paw volume in ml ± S.E.M. **P*< 0.05, ***P*< 0.01, ****P*< 0.001 as compared to saline treated group (one-way ANOVA followed by *post hoc* Dunnett's test), (*n* = 6 mice per group).

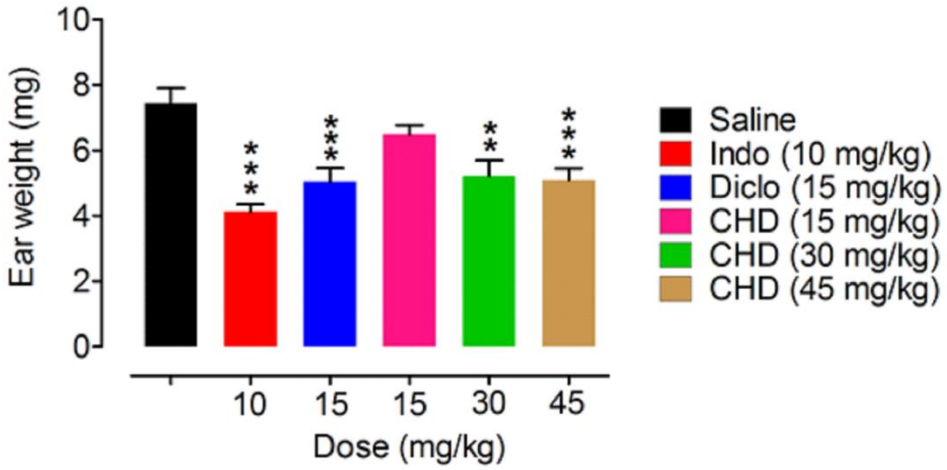

Fig. 11. Anti-inflammatory activity of CHD and the positive controls, indomethacin (Indo), and diclofenac (Diclo) in the xylene induced ear edema test. Each bar represents ear weight in mg ± S.E.M. **P*< 0.05, ***P*< 0.01, ****P*< 0.001 compared to the saline treated group (one-way ANOVA followed by *post hoc* Dunnett's test), (*n* = 6 mice per group).

3.3. In silico studies

3.3.1. Molecular Docking

Docking studies were performed to explore any possible underlying mechanism(s) of CHD anti-nociception and anti-inflammatory activity. Accordingly, simulations were carried out on: (1) cyclooxygenase-2 enzyme (COX-2), (2) GABA receptors and (3) opioid μ-, δ- and κ- receptors using Molecular Operating Environment (MOE 2016.08, Chemical Computing Group, Canada). Data concerning three-dimensional (3D) structures of enzymes with their co-crystalized ligands were downloaded from the Protein Data Bank (PDB) listed in Table 1 and the docking algorithm was validated by re-docking native co-crystalized ligands (Table 1). The computed root mean

square deviation (RMSD) between experimental and re-docked poses was found to be within a threshold limit < 2 Å.

The binding orientation of CHD and the native ligand into the binding site of the COX-2 isoform is shown in Figure 12A. The three-dimensional (3-D) interaction plot of CHD showed that the methoxy group formed a hydrogen bond interaction with His90, an important residue of a selectivity pocket. The carbonyl oxygen formed hydrogen bond interactions with Ala527 (Figure 12B). The computed binding energy for the CHD-COX-2 complex was -8.1050 kcal/mol and the docking score was -12.0458.

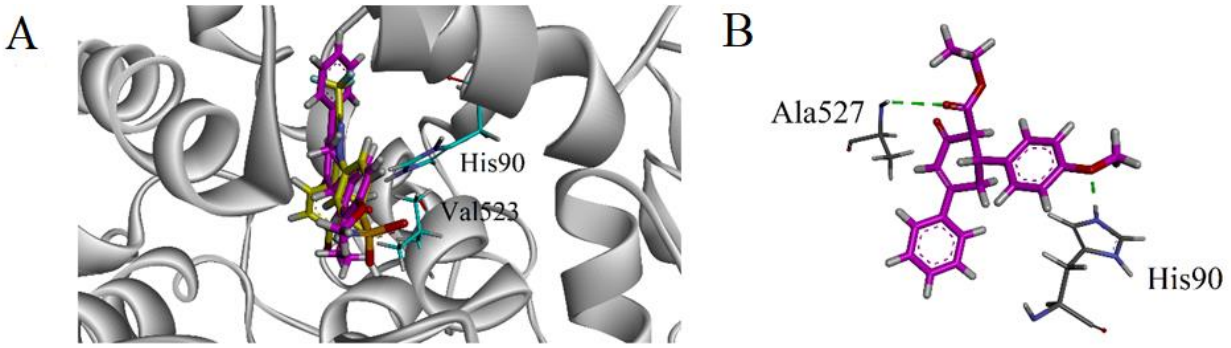

Fig. 12. (A) Ribbon diagram of overlaid binding orientation of CHD and native ligand into the binding site of the COX-2 enzyme. **(B)** Three-dimensional ligand-enzyme interaction plots of the cyclohexenone derivative (CHD) into the binding site of COX-2 enzyme.

For the GABA receptor, the docking study was carried out on PDB code 4COF (benzamidine). The computed binding energy for the ligand-$GABA_A$ complex was obtained as -5.4853 kcal/mol with a docking score of -8.4314. The superimposed three-dimensional ribbon model of the CHD, (purple), methaqualone (orange) (a positive allosteric $GABA_A$ receptor modulator) and native

ligand benzamidine (yellow) is shown in (Fig. 13). The 2D interaction plot showed that the phenyl ring of the synthesized compound creates π-π assembling interactions with Tyr62.

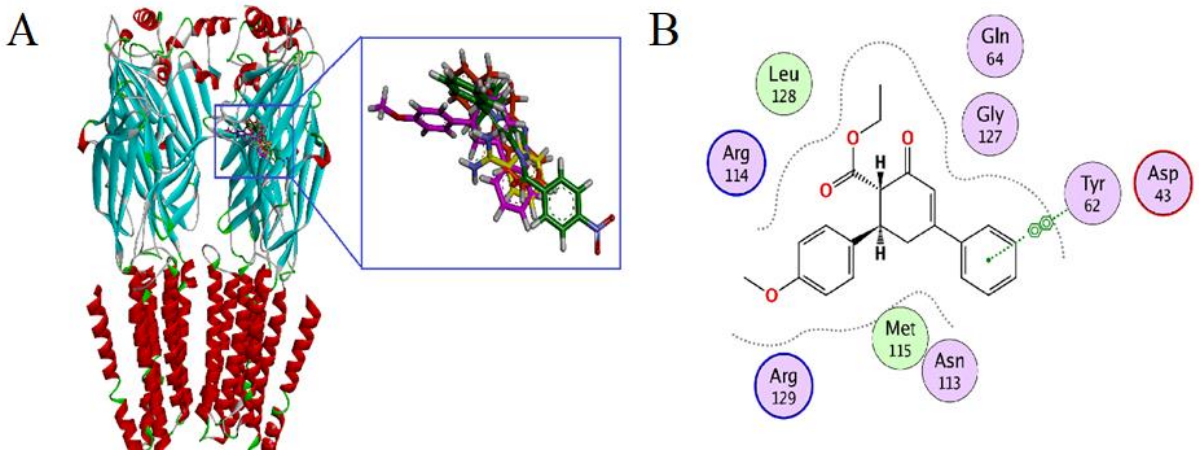

Fig. 13. (**A**) Three-dimensional superimposed binding pose of the native ligand benzamidine (yellow), cyclohexenone derivative (CHD; purple) and methaqualone (orange) into the binding site of the $GABA_A$ receptor (PDB code 4COF) and (**B**) Two-dimensional interaction plot for CHD.

For μ-opioid receptors (μOR), the computed binding affinity for the ligand-receptor complex was -7.0501 kcal/mol and the docking score was computed as -11.4240 (Fig. 14). μOR are important opioid receptors for pain perception and are currently the target of various potent centrally-acting analgesic drugs. The binding pose of CHD (purple) overlaid with β-funaltrexamine is shown in (Fig. 14). The ligand enzyme complex was stabilized by hydrophobic and π-sulfur interactions. The phenyl ring formed π-π stacking interactions with Tyr326, while the 4-methoxyphenyl group formed π-sulfur interactions with Met151.

The binding affinity and docking score in the case of the κ-opioid ligand-receptor complex was calculated as -8.0501 kcal/mol and -12.0240, respectively. The binding pose of the synthesized compound (purple) into the κ-opioid receptor active site (PDB code 4DJH) is shown in Fig. 14. CHD exhibited a binding pose similar to that of the co-crystalized ligand (JDC). The 3D interaction plot showed that the ligand-enzyme complex was stabilized by a hydrogen bond, hydrophobic, π-

560 sulfur as well as π-CH type interactions. Met142 formed π-sulfur interactions with the 4-
561 methoxyphenyl ring. The phenyl ring of CHD engages in π-π stacking interactions with Trp287.
562 A hydrogen bonding interaction was found between the carbonyl oxygen of the ring with Tyr312.
563 Similarly, Val108, Val230, Val290, Ile294 and Ile316 formed some π-alkyl interactions.

564 For the δ-opioid receptor, the binding affinity for the ligand-enzyme complex was calculated as -
565 7.4000 kcal/mol and the docking score was noted as -11.0903. In the case of δ-opioid receptors,
566 the 3D structure with naltrindole as co-crystalized ligand was retrieved (PDB code = 4EJ4). The
567 superimposed 3D binding pose of CHD (purple) with naltrindole (yellow) is shown in (Fig. 14).
568 The two-dimensional interaction plot showed that it interacted with Met132 *via* hydrogen bond
569 donor interactions.

570

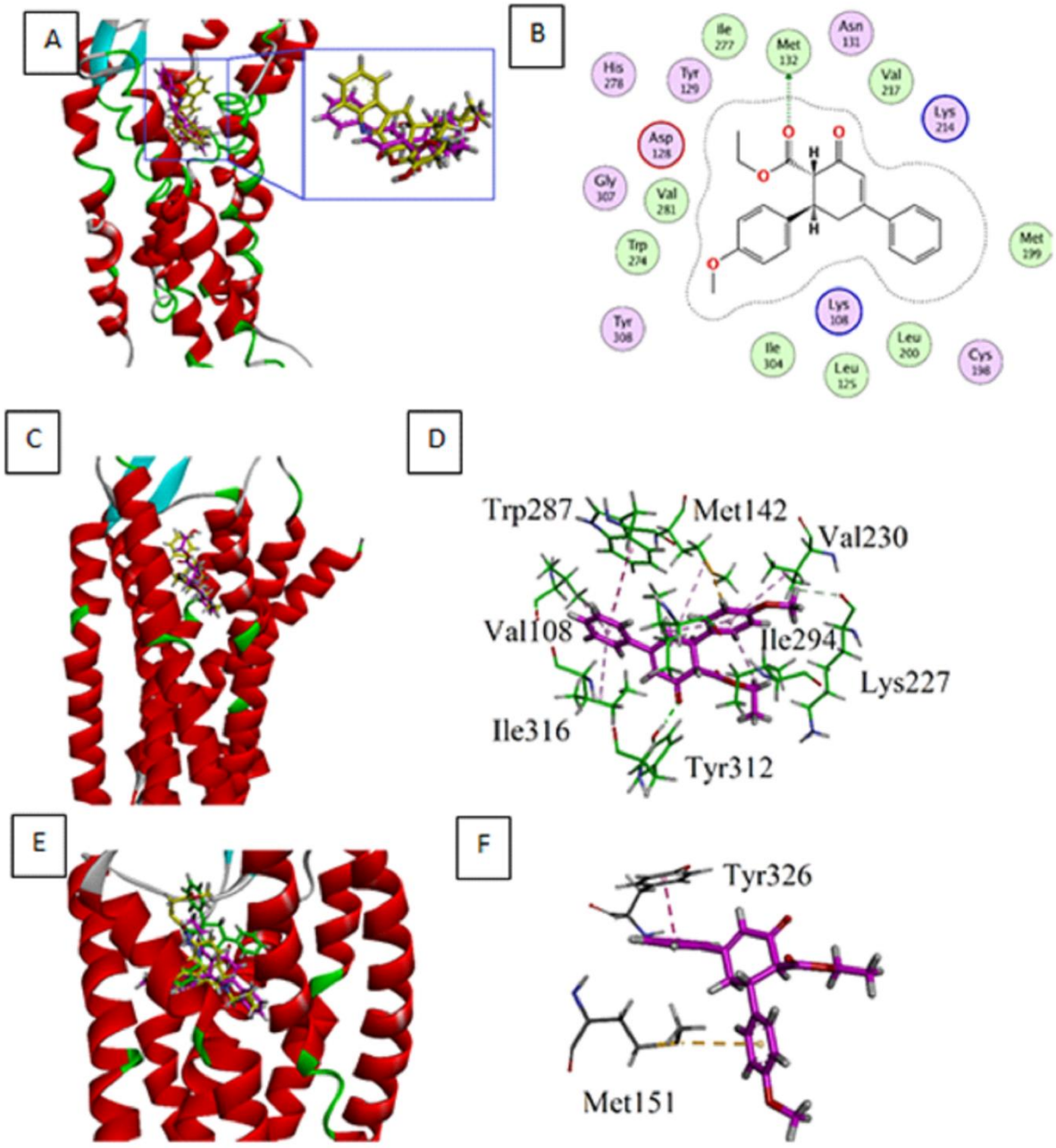

Fig. 14. Three and Two dimensional models of CHD binding with opioid receptors. (**A**) Three-dimensional and (**B**) Two-dimensional modeled superimposed binding pose of native ligand and CHD (purple) into the binding site of δ-opioid receptors (PDB code = 4EJ4). (**C**) Three-dimensional and (**D**) Two-dimensional model superimposed binding pose of native ligand and CHD (purple) into the binding site of κ-opioid receptor (PDB code = 4DJH). (**E**) Three-dimensional and (**F**) Two-dimensional model superimposed binding pose of the native ligand and selected compound CHD (purple) into the binding site of μ-opioid receptors (4DKL).

579

580 *3.3.2. Molecular Dynamics (MD) Simulations*

581 MD simulations were performed in order to understand the dynamics of all complexes and check
582 the stability of the CHD conformation at the docked site with respect to the backbone atoms for
583 each receptor. Among the complexes, 4COF, 1CX2, and 1EQG showed good stabilty in the
584 presence of CHD compared to the other three receptors (Fig. 15A). The mean RMSDs of these
585 were 2.0 Å, 2.4 Å, and 2.9 Å, respectively. These sites in the presence of CHD at the docked
586 position revealed very constant RMSD patterns throughout the simulaiton time, indicating a good
587 intermolecular strength of affinity and stability pattern. 4DJH (mean RMSD = 6.8 Å), 4DKL (mean
588 RMSD = 5.4 Å), and 4EJ4 (mean RMSD = 4.6 Å) showed major fluctuations in the receptor
589 structures, however, these changes do not affect the binding and conformation of the compound
590 with the receptors. In essence, these RMSD receptor fluctuations correspond to local protein
591 structure movments which are normal to their function. To substantiate compound conformation
592 stability, we additionally computed compound RMSDs in all complexes and plotted them versus
593 time. As can be seen in (Fig. 15B), the compounds were significantly stable with all receptor
594 RMSDs < 1 Å in all frames of the MD simulation.

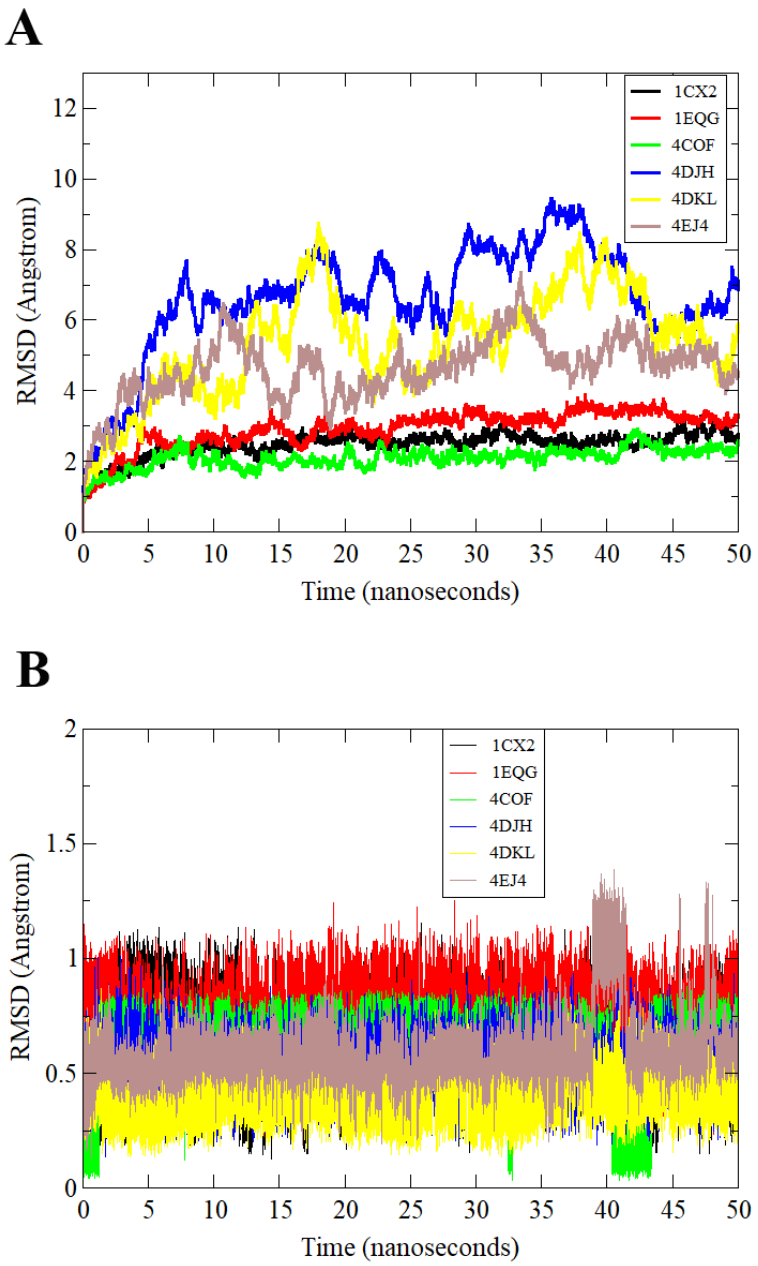

595

596 **Fig. 15.** (**A**) Root Mean Square Devitaions of backbone atoms for each receptor of docked
597 complexes. (**B**) CHD Root Mean Square Devitaions over 50-ns of MD simulation in complex with
598 receptors.

599

600

601

602 *3.3.1. MMPB/GBSA Binding Energy Calculation*

603 The free energy of binding was computed for all complexes to evaluate and revalidate the affinity
604 of intermolecular interactions and discover which type of interaction energy was dominant in
605 contributing to complex stability. All the complexes divulged robust interaction energies and were
606 dominated by gas phase energy in both MMGBSA and MMPBSA methodologies. Solvation
607 energy appeared to play less of a role in molecular interactions and was therefore non-favorable.
608 More specifically, the van der Waals energy of the gas phase disclosed by both methods played a
609 key role in complex stability whereas a minor contribution from electrostatic energy was also
610 evident except in the case of ICX2.The non-polar energy of solvation also favored docked
611 molecules as opposed to a highly unfavorable contribution from polar solvation energy. Overall,
612 the 4DKL receptor in complex with the CHD compound was highly stable with a MMGBSA
613 energy of -55.4492 kcal/mol and -47.9865 kcal/mol in MMPBSA. Details of MMGBSA and
614 MMPBSA energies of the complexes can be viewed in Table 4.

615

Table 4

MMGBSA and MMPBSA binding energies of the complexes

Method	Energy Component	1EQG	1CX2	4COF	4DKL	4EJ4	4DJH
MMGBSA	VDWAALS	-40.4511	-52.1322	-47.2564	-62.2517	-61.1760	-53.3142
	EEL	-6.2952	3.4110	-25.3784	-8.2760	-10.7373	-9.9464
	EGB	18.2375	8.9329	35.5743	21.3416	24.9894	19.8313
	ESURF	-4.3177	-5.6008	-4.8037	-6.2631	-6.2177	-5.5521
	DELTA G gas	-46.7463	-48.7212	-72.6348	-70.5277	-71.9133	-63.2606
	DELTA G solv	13.9198	3.3320	30.7706	15.0785	18.7716	14.2792
	DELTA TOTAL	-32.8265	-45.3892	-41.8641	-55.4492	-53.1417	-48.9814
MMPBSA	VDWAALS	-40.4511	-52.1322	-47.2564	-62.2517	-61.1760	-53.3142
	EEL	-6.2952	3.4110	-25.3784	-8.2760	-10.7373	-9.9464
	EPB	22.4009	14.6505	40.4885	26.2948	32.7712	26.3717
	ENPOLAR	-2.9491	-3.5859	-3.3982	-3.7537	-3.7336	-3.6908
	EDISPER	0.0000	0.0000	0.0000	0.0000	0.0000	0.0000
	DELTA G gas	-46.7463	-48.7212	-72.6348	-70.5277	-71.9133	-63.2606
	DELTA G solv	19.4518	11.0646	37.0904	22.5411	29.0376	22.6810
	DELTA TOTAL	-27.2945	-37.6567	-35.5444	-47.9865	-42.8757	-40.5796

4. Discussion

Cyclohexenone derivatives have received considerable attention over recent years not only preclinically, but also clinically because of their extensive pharmacological possibilities. These include: analgesic (Said et al., 2009), anti-inflammatory (Yaouba et al., 2018), anti-neuropathic (Khan et al., 2019), antipyretic (Mousavi, 2016), antibacterial (Saranya and Ravi, 2012), antioxidant (Okoth et al., 2016), antifungal (Kanagarajan et al., 2013), antimalarial (Ledoux et al.,

626 2017), anti-tubercular (Monga et al., 2014), anti-leishmanial (Das and Manna, 2015),
627 anticonvulsant (Said et al., 2009) tyrosine kinase inhibitory (Nazar et al., 2015) cytotoxic (Ayyad
628 et al., 1998) and anticancer (Okoth and Koorbanally, 2015) activities. Bearing in mind these wide-
629 ranging potential capacities of cyclohexenone functionality, this study was designed to examine a
630 selected cyclohexanone derivative (CHD) exemplar (Ethyl 6-(4-metohxyphenyl)-2-oxo-4-
631 phenylcyclohexe-3-enecarboxylate). This was done firstly for its safety profile; secondly, to
632 investigate any feasible *in vivo* effects in standard animal models of nociceptive and inflammatory
633 pain; thirdly, to perform molecular docking and molecular dynamic (MD) simulation studies to
634 facilitate interpretation of targeted drug-receptor interactions to corroborate the *in vivo* findings.
635 In parallel with this research approach, *in vitro* assays were conducted to examine any possibility
636 of COX-2 or 5-LOX enzyme inhibition and/or suppression of mRNA expression of TNF-α, IL-1β
637 and COX-2 that might underlie anti-nociceptive and anti-inflammatory effects.

638 Four nociceptive and inflammatory, highly reproducible standard models were used to generate
639 the results. The findings clearly indicated that CHD possessed a noteworthy degree of safety with
640 a maximum tolerated dose above 240 mg/kg. Statistically significant anti-nociceptive and anti-
641 inflammatory activity was found in the rodent models. These effects were comparable to those of
642 aspirin, tramadol, indomethacin and diclofenac used as positive controls (Figs. 3, 4, 5, 6, 7, 8, 9,
643 10 and 11). Moreover, *in silico* docking analysis demonstrated that CHD manifested
644 favorable interactions with common pain targets i.e. COX-1/2 enzymes in addition to opioid and
645 $GABA_A$ receptors (Figs. 12, 13 and 14.) substantiating the in-vivo results. Equally, CHD produced
646 marked inhibition of COX-2 and 5-LOX in the enzyme assays while in the case of RT-PCR, CHD
647 reduced the mRNA expression of TNF-α, IL-1β and COX-2.

Administration of GABA receptor agonists either supraspinally, spinally or peripherally, has been reported to reduce the nociceptive index in models of neuropathic and inflammatory pain (Malan et al., 2002; Patel et al., 2001). In our study, it is postulated that CHD alleviates centrally mediated nociception via GABAergic and opioidergic mechanisms (Fig. 7) alongside a capability of interaction with the COX-1/2 target (Fig. 12). An involvement of GABAergic and opioidergic systems was further reinforced by computational studies whereby CHD exhibited favorable binding affinity for the $GABA_A$ (Fig. 13) and opioid receptor subtypes (μ, κ and δ) (Fig. 14). It has been reported that GABAergic agonists may augment the anti-nociceptive effect of a centrally acting analgesic such as morphine (Sawynok, 1984), hence, it is conceivable that GABA receptor agonist administration may represent a therapeutic option for the management of both chronic and acute pain (McCarson and Enna, 2014) or as a combination of GABA with opioid receptor related therapies.

The acetic acid induced abdominal constriction assay is a tonic visceral pain model frequently utilized for monitoring the anti-nociceptive action of drugs (Utsunomiya et al., 1998). Although it is a very sensitive test, it cannot distinguish whether the nociceptive activity is peripherally or centrally mediated (Chen et al., 1995). It entails stimulation of visceral receptors followed by the release of bradykinin, serotonin, cyclooxygenase, prostaglandins and interleukins which induce pain and inflammation (Olonode et al., 2015; Rodrigues et al., 2012). It also implicates an enhanced activation of peripheral receptors (Bentley et al., 1983) and innervated nociceptive nerve terminals (Duarte et al., 1988). In the current study, CHD induced a significant reduction in abdominal constrictions in a dose-dependent manner comparable to standard aspirin (Fig. 3A-B).

Hot plate and tail immersion nociceptive tests were employed to determine the central anti-nociceptive potential of CHD. These models can specifically evaluate possible central nociception

(Eddy and Leimbach, 1953), where there is a non-inflammatory and acute nociceptive reaction developed upon exposure to heat via spinal receptors which is evidence of centrally mediated anti-nociception (Amabeoku and Kabatende, 2012; Pini et al., 1997). CHD moderately enhanced the hot plate latencies of mice compared to standard tramadol, suggesting it to be a centrally acting analgesic (Fig. 4). In the tail immersion test, the behavioural response is predominantly controlled by supraspinal and spinal entities (Danneman et al., 1994). At the doses studied, CHD presented a modest increase in tail withdrawal latency, but tramadol produced a more pronounced latency elevation (Fig. 5). The duration of action of a drug depends on several factors including biological half-life, first pass effect, plasma protein binding and other pharmacokinetic factors, nature of formulation, co-morbid conditions such as renal impairment or liver disfunction. Any of the above cited factors, may be a potential contributor to the loss of CHD effectiveness at the doses of 30 and 45 mg/kg in the thermal nociception tests within 90 min (hot plate test) and 120 min (tail immersion test), respectively. The formalin induced nociceptive paradigm comprises of a binary phased nociceptive reaction and neuropathic pain (Salinas-Abarca et al., 2017). A neurogenic or first phase (0-5 min) in which class C fibres are stimulated and an inflammatory or second phase (10 to 30 min) which involves the release of inflammatory mediators (Hunskaar and Hole, 1987; Tjølsen et al., 1992). Interestingly, CHD was effective in both the neurogenic and inflammatory mediator phases (Fig. 6), further reinforcing the concept of a possible centrally acting anti-nociceptive component mechanism in the activity of this compound. Moreover, in experiments involving pharmacological antagonism of CHD anti-nociception with PTZ and naloxone, it was divulged that an apparent participation of both GABAergic and opioidergic mechanisms was implicated (Fig. 7A-B).

693 The anti-inflammatory activity of CHD was investigated by employing four standard models
694 of inflammation i.e., the carrageenan, serotonin, histamine and xylene mediated edema tests (Figs.
695 8, 9, 10 and 11). The carrageenan incited paw volume model is most extensively employed for
696 evaluating the anti-edematous potential of drugs (Mazzanti and Braghiroli, 1994). Localised paw
697 injection of carrageenan in mice initiates a three-phased inflammatory process. The primary phase
698 (0 to 1.5 h), is caused by the release of serotonin and histamine whereas the secondary phase (1.5
699 to 2.5 h) is mediated via bradykinin and the tertiary phase (2.5 to 5 h) is elicited mainly by the
700 generation of prostaglandins (Suba et al., 2005).

701 CHD (15 - 45 mg/kg) substantially reduced the elevated paw edema in all three phases of the
702 carrageenan-induced paw volume assay and this was comparable to the response yielded by the
703 standard drug, aspirin (Fig 8A-B). In order to authenticate the finding from the carrageenan paw
704 edema model, the anti-edematous effect of CHD was further investigated in the three other
705 standard models (histamine and serotonin induced paw volume and xylene induced ear edema).
706 Histamine and serotonin can increase vascular permeability and both are effective vasodilators
707 (Skidmore and Whitehouse, 1967) which are conducive to an ensuing edema. CHD not only
708 suppressed the edema mediated by histamine and serotonin but also that of xylene at doses
709 corresponding to standard anti-inflammatory drugs (Figs. 9A-B, 10A-B and 11). The xylene
710 induced ear edema model is extensively utilized to determine the anti-inflammatory action of
711 steroidal and non-steroidal anti-phlogistic agents (Zanini Jr et al., 1992). Studies reported in the
712 literature have revealed that xylene also promotes vascular permeability causing skin edema owing
713 to the release of inflammatory mediators leading to acute neurogenic inflammation (Bánki et al.,
714 2014). CHD markedly reduced ear edema induced by xylene comparable to the standard agents
715 (Fig. 11).

To further corroborate the anti-nociceptive and anti-inflammatory potential of CHD, it was subjected to *in vitro* studies involving 5-LOX and COX-2 enzyme inhibition assays along with RT-PCR studies. Thus, CHD substantially inhibited 5-LOX and COX-2 enzymes in comparison with the standard inhibitors zileuton and celecoxib respectively as shown in (Table 2 and 3). In the case of RT-PCR studies, CHD decreased the mRNA expression of COX-2, TNF-α and IL-1β compared to the carrageenan treated control group as presented in Fig. 2. This *in vitro* study therefore endorsed the promising anti-nociceptive and anti-inflammatory findings with CHD in both the *in vivo* and *in silico* studies which further strengthens a potential for application in pain and inflammation.

In summary, *in silico* docking analysis demonstrated that the synthesized cyclohexanone derivative has shown favourable interactions with common pain targets i.e. COX 1/2, $GABA_A$ and opioid receptors (Figs. 12, 13 and 14). The binding affinity study revealed that the intensity of interactions of the CHD ligand with the COX-2 isozyme was more than that with COX-1 and this was supported by the degree of 5-LOX and COX-2 enzyme inhibition observed (Table 2 and 3). In addition, MD simulations of the complexes revealed that CHD was a highly stable molecule at the docked site and generated robust chemical interactions underlying strong intermolecular affinity (Table 4). Interactions with other pharmacological targets suggest that CHD may act as a novel nociceptive and inflammatory pain reliever supported by *in vivo* studies (Figs. 3, 4, 5, 6, 7, 8, 9, 10 and 11).

5. Conclusions

This study elucidated the synthesis and pharmacological evaluation of a novel cyclohexenone derivative (CHD) as a putative analgesic agent. CHD possessed not only anti-nociceptive, but also anti-inflammatory activity when tested in validated models of pain and inflammation in mice.

These *in vivo* properties were attended by an inhibitory action on COX-2 and 5-LOX enzymes *in vitro* in addition to a complementary *in silico* interaction with $GABA_A$ and opioid receptors. Consequently, CHD represents an innovative and noteworthy anti-nociceptive and anti-inflammatory compound worthy of further pharmacological investigation and possible development.

Acknowledgments

Dr. Umer Rashid is grateful to the Higher Education Commission of Pakistan for budgetary support for purchasing an MOE license under HEC-NRPU project 5291/Federal/NRPU/R&D/HEC/2016. The selected compound under study has been synthesized as a part of series of compounds with confirmed structures by Dr. Rasool Khan, Associate Professor, Institute of Chemical Science, University of Peshawar. We are grateful to him for providing a series of compounds and after preliminary study, we selected the cited compound (CHD) for our study.

Conflict of interest

The authors have no conflict of interest.

Authors' contributions

GA conceived the research study and directed the research group as supervisor of the pharmacological experimentation. GA also interpreted the results in addition to critically reviewing the contents of the final version of manuscript. JK carried out the pharmacological experiments and performed the statistical analyses. He likewise developed the preliminary draft of the manuscript. RK helped in planning and supervising experiments related to the chemistry of our

selected compound. UR conducted the computational studies and performed related calculations, interpretations and analysis. RU, MSJ, AAK, SA and SA helped in conducting the in vitro and in silico studies. All authors read and approved the final manuscript and RDES had an intellectual input in the writing of the manuscript and the interpretational outcome of the study.

References

Abbas, M., Subhan, F., Mohani, N., Rauf, K., Ali, G., Khan, M., 2011. The involvement of opioidergic mechanisms in the activity of Bacopa monnieriextract and its toxicological studies. Afr. J. Pharm. Pharmacol. 5, 1120-1124.

Abbasi, S., Raza, S., Azam, S.S., Liedl, K.R., Fuchs, J.E., 2016. Interaction mechanisms of a melatonergic inhibitor in the melatonin synthesis pathway. J. Mol. Liq. 221, 507-517.

Abro, A., Azam, S.S., 2016. Binding free energy based analysis of arsenic (+ 3 oxidation state) methyltransferase with S-adenosylmethionine. J. Mol. Liq. 220, 375-382.

Ahmad, N., Subhan, F., Islam, N.U., Shahid, M., Rahman, F.U., Sewell, R.D.J.E.j.o.p., 2017. Gabapentin and its salicylaldehyde derivative alleviate allodynia and hypoalgesia in a cisplatin-induced neuropathic pain model. Eur. J. Pharmacol. 814, 302-312.

Ahmadi, A., Khalili, M., Hajikhani, R., Hosseini, H., Afshin, N., Nahri-Niknafs, B., 2012. Synthesis and study the analgesic effects of new analogues of ketamine on female wistar rats. Med. Chem. 8, 246-251.

Akbar, S., Subhan, F., Karim, N., Shahid, M., Ahmad, N., Ali, G., Mahmood, W., Fawad, K.J.B., Pharmacotherapy, 2016. 6-Methoxyflavanone attenuates mechanical allodynia and vulvodynia in the streptozotocin-induced diabetic neuropathic pain. Biomed. Pharmacother. 84, 962-971.

Ali, G., Subhan, F., Abbas, M., Zeb, J., Shahid, M., Sewell, R.D., 2015. A streptozotocin-induced diabetic neuropathic pain model for static or dynamic mechanical allodynia and vulvodynia: validation using topical and systemic gabapentin. Naunyn-Schmiedeberg's. Arch. Pharmacol. 388, 1129-1140.

785 Ali, G., Subhan, F., Wadood, A., Ullah, N., Islam, N.U., Khan, I., 2013. Pharmacological evaluation,
786 molecular docking and dynamics simulation studies of salicyl alcohol nitrogen containing derivatives. Afr.
787 J. Pharm. Pharmacol. 7, 585-596.
788 Almeer, R.S., Hammad, S.F., Leheta, O.F., Abdel Moneim, A.E., Amin, H.K., 2019. Anti-inflammatory and
789 anti-hyperuricemic functions of two synthetic hybrid drugs with dual biological active sites. Int. J. Mol. Sci.
790 20, 5635.
791 Amabeoku, G.J., Kabatende, J., 2012. Antinociceptive and anti-inflammatory activities of leaf methanol
792 extract of Cotyledon orbiculata L.(Crassulaceae). Adv. Pharmacol. Sci. 2012, 5-6.
793 Ayyad, S.-E.N., Judd, A.S., Shier, W.T., Hoye, T.R., 1998. Otteliones A and B: Potently cytotoxic 4-
794 methylene-2-cyclohexenones from Ottelia alismoides. J. Org. Chem. 63, 8102-8106.
795 Bánki, E., Hajna, Z., Kemeny, A., Botz, B., Nagy, P., Bolcskei, K., Tóth, G., Reglodi, D., Helyes, Z., 2014. The
796 selective PAC1 receptor agonist maxadilan inhibits neurogenic vasodilation and edema formation in the
797 mouse skin. Neuropharmacology 85, 538-547.
798 Bentley, G., Newton, S., Starr, J., 1983. Studies on the antinociceptive action of α-agonist drugs and their
799 interactions with opioid mechanisms. Br. J. Pharmacol. 79, 125-134.
800 Burnett, B., Jia, Q., Zhao, Y., Levy, R., 2007. A medicinal extract of Scutellaria baicalensis and Acacia
801 catechu acts as a dual inhibitor of cyclooxygenase and 5-lipoxygenase to reduce inflammation. J. Med.
802 Food. 10, 442-451.
803 Case, D., Darden, T., Cheatham III, T., Simmerling, C., Wang, J., Duke, R., Luo, R., Walker, R., Zhang, W.,
804 Merz, K., 2010. AMBER 12; University of California: San Francisco, 2012. There is no corresponding record
805 for this reference.[Google Scholar], 1-826.
806 Chapman, C.R., Gavrin, J., 1999. Suffering: the contributions of persistent pain. Lancet 353, 2233-2237.
807 Chen, Y.-F., Tsai, H.-Y., Wu, T.-S., 1995. Anti-inflammatory and analgesic activities from roots of Angelica
808 pubescens. Planta. Med. 61, 2-8.

809 Cheon, M.S., Yoon, T., Choi, G., Moon, B.C., Lee, A.-Y., Choo, B.K., Kim, H.K., 2009. Chrysanthemum
810 indicum Linné extract inhibits the inflammatory response by suppressing NF-κB and MAPKs activation in
811 lipopolysaccharide-induced RAW 264.7 macrophages. J. Ethnopharmacol. 122, 473-477.
812 Danneman, P.J., Kiritsy-Roy, J.A., Morrow, T.J., Casey, K.L., 1994. Central delay of the laser-activated rat
813 tail-flick reflex. Pain 58, 39-44.
814 Das, M., Manna, K., 2015. Bioactive cyclohexenones: a mini review. Curr. Bioact. Compd. 11, 239-248.
815 DiMasi, J.A., Feldman, L., Seckler, A., Wilson, A., 2010. Trends in risks associated with new drug
816 development: success rates for investigational drugs. Clin. Pharmacol. Ther. 87, 272-277.
817 Duarte, I., Nakamura, M., Ferreira, S., 1988. Participation of the sympathetic system in acetic acid-induced
818 writhing in mice. Braz. J. Med. Biol. Res. 21, 341-343.
819 Eddy, N.B., Leimbach, D., 1953. Synthetic analgesics. II. Dithienylbutenyl-and dithienylbutylamines. J.
820 Pharmacol. Exp. Ther. 107, 385-393.
821 Fang, S.-M., Cui, C.-B., Li, C.-W., Wu, C.-J., Zhang, Z.-J., Li, L., Huang, X.-J., Ye, W.-C., 2012.
822 Purpurogemutantin and purpurogemutantidin, new drimenyl cyclohexenone derivatives produced by a
823 mutant obtained by diethyl sulfate mutagenesis of a marine-derived Penicillium purpurogenum G59. Mar.
824 Drugs. 10, 1266-1287.
825 Fawad, K., Islam, N.U., Subhan, F., Shahid, M., Ali, G., Rahman, F.-U., Mahmood, W., Ahmad, N., 2018.
826 Novel hydroquinone derivatives alleviate algesia, inflammation and pyrexia in the absence of gastric
827 ulcerogenicity. Trop. J. Pharm. Res. 17, 53-63.
828 Fernandes, J.V., Cobucci, R.N.O., Jatobá, C.A.N., de Medeiros Fernandes, T.A.A., de Azevedo, J.W.V., de
829 Araújo, J.M.G., 2015. The role of the mediators of inflammation in cancer development. Pathol. Oncol.
830 Res. 21, 527-534.

831 Gopalakrishnan, M., Thanusu, J., Kanagarajan, V., 2008. Synthesis and characterization of 4, 6-diaryl-4, 5-
832 dihydro-2H-indazol-3-ols and 4, 6-diaryl-2-phenyl-4, 5-dihydro-2H-indazol-3-ols—a new series of fused
833 indazole derivatives. Chem. Heterocycl. Comp. 44, 950-955.
834 Gutthann, S.P., Rodríguez, L.A.G., Raiford, D.S., Oliart, A.D., Romeu, J.R., 1996. Nonsteroidal anti-
835 inflammatory drugs and the risk of hospitalization for acute renal failure. Arch. Intern. Med. 156, 2433-
836 2439.
837 Hunskaar, S., Hole, K., 1987. The formalin test in mice: dissociation between inflammatory and non-
838 inflammatory pain. Pain 30, 103-114.
839 Iftikhar, F., Ali, Y., Kiani, F.A., Hassan, S.F., Fatima, T., Khan, A., Niaz, B., Hassan, A., Ansari, F.L., Rashid, U.,
840 2017. Design, synthesis, in vitro Evaluation and docking studies on dihydropyrimidine-based urease
841 inhibitors. Bioorg. Chem. 74, 53-65.
842 Iftikhar, F., Yoqoob, F., Tabassum, N., Jan, M.S., Sadiq, A., Tahir, S., Batool, T., Niaz, B., Ansari, F.L.,
843 Chaudhary, M.I., 2018. Design, Synthesis, In-Vitro Thymidine Phosphorylase Inhibition, In-Vivo
844 Antiangiogenic and In-Silico Studies of C-6 substituted dihydropyrimidines. Bioorg. Chem. 80, 99-111.
845 Islam, N.U., Amin, R., Shahid, M., Amin, M., Zaib, S., Iqbal, J., 2017. A multi-target therapeutic potential of
846 Prunus domestica gum stabilized nanoparticles exhibited prospective anticancer, antibacterial, urease-
847 inhibition, anti-inflammatory and analgesic properties. BMC. Complement. Altern. Med. 17, 272-276.
848 Islam, N.U., Jalil, K., Shahid, M., Rauf, A., Muhammad, N., Khan, A., Shah, M.R., Khan, M.A., 2019. Green
849 synthesis and biological activities of gold nanoparticles functionalized with Salix alba. Arab. J. Chem. 12,
850 2914-2925.
851 Jan, M.S., Ahmad, S., Hussain, F., Ahmad, A., Mahmood, F., Rashid, U., Ullah, F., Ayaz, M., Sadiq,
852 A.J.E.j.o.m.c., 2020. Design, synthesis, in-vitro, in-vivo and in-silico studies of pyrrolidine-2, 5-dione
853 derivatives as multitarget anti-inflammatory agents. Eur. J. Med. Chem. 186, 111863.

Johnson, T., Pultar, F., Menke, F., Lautens, M., 2016. Palladium-Catalyzed α-Arylation of Vinylogous Esters for the Synthesis of γ, γ-Disubstituted Cyclohexenones. Org. Lett. 18, 6488-6491.

Jones, R., Rubin, G., Berenbaum, F., Scheiman, J., 2008. Gastrointestinal and cardiovascular risks of nonsteroidal anti-inflammatory drugs. Am. J. Med. 121, 464-474.

Kanagarajan, V., Ezhilarasi, M., Bhakiaraj, D., Gopalakrishnan, M., 2013. In vitro anticandidal evaluation of novel highly functionalized bis cyclohexenone ethyl carboxylates. Eur. Rev. Med. Pharmacol. Sci. 17, 292-298.

Khalid, S., Ullah, M.Z., Khan, A.U., Afridi, R., Rasheed, H., Khan, A., Ali, H., Kim, Y.S., Khan, S., 2018. Antihyperalgesic properties of honokiol in inflammatory pain models by targeting of NF-κB and Nrf2 signaling. Front Pharmacol. 9, 140.

Khan, J., Ali, G., Khan, R., Ullah, R., Ullah, S., 2019. Attenuation of vincristine-induced neuropathy by synthetic cyclohexenone-functionalized derivative in mice model. Neurol Sci, 1-13.

Kidd, B., Urban, L., 2001. Mechanisms of inflammatory pain. Br. J. Anaesth. 87, 3-11.

Laxmaiah Manchikanti, M., Bert Fellows, M., Hary Ailinani, M., 2010. Therapeutic use, abuse, and nonmedical use of opioids: a ten-year perspective. Pain. Physician. 13, 401-435.

Lednicer, D., Von Voigtlander, P.F., Emmert, D.E., 1981a. 4-Aryl-4-aminocyclohexanones and their derivatives, a novel class of analgesics. 3. m-hydroxyphenyl derivatives. J. Med. Chem. 24, 341-346.

Lednicer, D., VonVoigtlander, P.F., Emmert, D.E., 1981b. 4-Amino-4-arylcyclohexanones and their derivatives: a novel class of analgesics. 2. Modification of the carbonyl function. J. Med. Chem. 24, 404-408.

Ledoux, A., St-Gelais, A., Cieckiewicz, E., Jansen, O., Bordignon, A., Illien, B., Di Giovanni, N., Marvilliers, A., Hoareau, F., Pendeville, H., 2017. Antimalarial activities of alkyl cyclohexenone derivatives isolated from the leaves of Poupartia borbonica. J. Nat. Prod. 80, 1750-1757.

877 Liu, D., Yu, W., Li, J., Pang, C., Zhao, L., 2013. Novel 2-(E)-substituted benzylidene-6-(N-substituted
878 aminomethyl) cyclohexanones and cyclohexanols as analgesic and anti-inflammatory agents. Med. Chem.
879 Res. 22, 3779-3786.
880 Malan, T.P., Mata, H.P., Porreca, F., 2002. Spinal GABAAand GABABReceptor Pharmacology in a Rat Model
881 of Neuropathic Pain. Anesthesiology. 96, 1161-1167.
882 Manouze, H., Bouchatta, O., Gadhi, A.C., Bennis, M., Sokar, Z., Ba-M'hamed, S., 2017. Anti-inflammatory,
883 antinociceptive, and antioxidant activities of methanol and aqueous extracts of Anacyclus pyrethrum
884 roots. Front. Pharmacol. 8, 592-598.
885 Masresha, B., Makonnen, E., Debella, A., 2012. In vivo anti-inflammatory activities of Ocimum suave in
886 mice. J. Ethnopharmacol. 142, 201-205.
887 Mayer, D.J., Mao, J., Price, D.D., 1995. The development of morphine tolerance and dependence is
888 associated with translocation of protein kinase C. Pain 61, 365-374.
889 Mazzanti, G., Braghiroli, L., 1994. Analgesic antiinflammatory action of Pfaffia paniculata (Martius) kuntze.
890 Phytother Res 8, 413-416.
891 McCarson, K.E., Enna, S., 2014. GABA pharmacology: the search for analgesics. Neurochem. Res. 39, 1948-
892 1963.
893 Mequanint, W., Makonnen, E., Urga, K., 2011. In vivo anti-inflammatory activities of leaf extracts of
894 Ocimum lamiifolium in mice model. J. Ethnopharmacol. 134, 32-36.
895 Miller III, B.R., McGee Jr, T.D., Swails, J.M., Homeyer, N., Gohlke, H., Roitberg, A.E., 2012. MMPBSA. py: an
896 efficient program for end-state free energy calculations. J. Chem. Theory. Comput. 8, 3314-3321.
897 Ming-Tatt, L., Khalivulla, S.I., Akhtar, M.N., Lajis, N., Perimal, E.K., Akira, A., Ali, D.I., Sulaiman, M.R., 2013.
898 Anti-Hyperalgesic effect of a benzilidine-cyclohexanone analogue on a mouse model of chronic
899 constriction injury-induced neuropathic pain: Participation of the κ-Opioid receptor and KATP. Pharmacol.
900 Biochem. Behav. 114, 58-63.

Ming-Tatt, L., Khalivulla, S.I., Akhtar, M.N., Mohamad, A.S., Perimal, E.K., Khalid, M.H., Akira, A., Lajis, N., Israf, D.A., Sulaiman, M.R., 2012. Antinociceptive Activity of a Synthetic Curcuminoid Analogue, 2, 6-bis-(4-hydroxy-3-methoxybenzylidene) cyclohexanone, on Nociception-induced Models in Mice. Basic Clin. Pharmacol. Toxicol. 110, 275-282.

Monga, V., Goyal, K., Steindel, M., Malhotra, M., Rajani, D.P., Rajani, S.D., 2014. Synthesis and evaluation of new chalcones, derived pyrazoline and cyclohexenone derivatives as potent antimicrobial, antitubercular and antileishmanial agents. Med. Chem. Res. 23, 2019-2032.

Mousavi, S.R., 2016. Claisen–Schmidt condensation: Synthesis of (1S, 6R)/(1R, 6S)-2-oxo-N, 4, 6-triarylcyclohex-3-enecarboxamide derivatives with different substituents in H2O/EtOH. Chirality 28, 728-736.

Muhammad, N., Saeed, M., Khan, H., 2012. Antipyretic, analgesic and anti-inflammatory activity of Viola betonicifolia whole plant. BMC. Complement. Altern. Med. 12, 53-59.

Nazar, M.F., Abdullah, M.I., Badshah, A., Mahmood, A., Rana, U.A., Khan, S.U.-D., 2015. Synthesis, structure–activity relationship and molecular docking of cyclohexenone based analogous as potent non-nucleoside reverse-transcriptase inhibitors. J. Mol. Struct. 1086, 8-16.

Okoth, D.A., Akala, H.M., Johnson, J.D., Koorbanally, N.A., 2016. Alkyl phenols, alkenyl cyclohexenones and other phytochemical constituents from Lannea rivae (chiov) Sacleux (Anacardiaceae) and their bioactivity. Med. Chem. Res. 25, 690-703.

Okoth, D.A., Koorbanally, N.A., 2015. Cardanols, long chain cyclohexenones and cyclohexenols from Lannea schimperi (Anacardiaceae). Nat. Prod. Commun. 10, 103-106.

Olonode, E.T., Aderibigbe, A.O., Bakre, A.G., 2015. Anti-nociceptive activity of the crude extract of Myrianthus arboreus P. Beauv (Cecropiaceae) in mice. J Ethnopharmacol 171, 94-98.

923 Patel, S., Naeem, S., Kesingland, A., Froestl, W., Capogna, M., Urban, L., Fox, A., 2001. The effects of GABAB
924 agonists and gabapentin on mechanical hyperalgesia in models of neuropathic and inflammatory pain in
925 the rat. Pain 90, 217-226.
926 Pini, L.A., Vitale, G., Ottani, A., Sandrini, M., 1997. Naloxone-reversible antinociception by paracetamol in
927 the rat. J. Pharmacol. Exp. Ther. 280, 934-940.
928 Rashid, U., Sultana, R., Shaheen, N., Hassan, S.F., Yaqoob, F., Ahmad, M.J., Iftikhar, F., Sultana, N., Asghar,
929 S., Yasinzai, M., 2016. Structure based medicinal chemistry-driven strategy to design substituted
930 dihydropyrimidines as potential antileishmanial agents. Eur. J. Med. Chem. 115, 230-244.
931 Rodrigues, M.R.A., Kanazawa, L.K.S., das Neves, T.L.M., da Silva, C.F., Horst, H., Pizzolatti, M.G., Santos,
932 A.R.S., Baggio, C.H., de Paula Werner, M.F., 2012. Antinociceptive and anti-inflammatory potential of
933 extract and isolated compounds from the leaves of Salvia officinalis in mice. J. Ethnopharmacol. 139, 519-
934 526.
935 Rukh, L., Ali, G., Ullah, R., Islam, N.U., Shahid, M.J.E.J.o.P., 2020. Efficacy assessment of salicylidene
936 salicylhydrazide in chemotherapy associated peripheral neuropathy. Eur. J. Pharmacol. 888, 173481.
937 Said, S.A., Amr, A.E.-G.E., Sabry, N.M., Abdalla, M.M., 2009. Analgesic, anticonvulsant and anti-
938 inflammatory activities of some synthesized benzodiazipine, triazolopyrimidine and bis-imide derivatives.
939 Eur. J. Med. Chem. 44, 4787-4792.
940 Salinas-Abarca, A.B., Avila-Rojas, S.H., Barragán-Iglesias, P., Pineda-Farias, J.B., Granados-Soto, V.J.E.j.o.p.,
941 2017. Formalin injection produces long-lasting hypersensitivity with characteristics of neuropathic pain.
942 Eur. J. Pharmacol. 797, 83-93.
943 Saranya, A.V., Ravi, S., 2012. Synthesis, Characterization and Anti-bacterial activity of pyrimidine,
944 cyclohexenone and 1, 5-diketone derivatives of Furfural Chalcone. J. Pharm. Res. 5, 1098-1101.
945 Sawynok, J., 1984. GABAergic mechanisms in antinociception. Prog. Neuropsychopharmacol. Biol.
946 Psychiatry. 8, 581-586.

947 Senguttuvan, S., Nagarajan, S., 2010. Synthesis of 2-amino-5-aryl-5, 6-dihydro-7-(naphthalen-2-yl)
948 quinazolin-4-ols. Int. J. Chem. 2, 108.
949 Sewell, R., Spencer, P., 1976. Antinociceptive activity of narcotic agonist and partial agonist analgesics and
950 other agents in the tail-immersion test in mice and rats. Neuropharmacology. 15, 683-688.
951 Shahid, M., Subhan, F., Ahmad, N., Ali, G., Akbar, S., Fawad, K., Sewell, R., 2017a. Topical gabapentin gel
952 alleviates allodynia and hyperalgesia in the chronic sciatic nerve constriction injury neuropathic pain
953 model. Eur. J. Pain. 21, 668-680.
954 Shahid, M., Subhan, F., Ahmad, N., Ullah, I., 2017b. A bacosides containing Bacopa monnieri extract
955 alleviates allodynia and hyperalgesia in the chronic constriction injury model of neuropathic pain in rats.
956 BMC. Complement. Altern. Med. 17, 293.
957 Shahid, M., Subhan, F., Ullah, I., Ali, G., Alam, J., Shah, R., 2016. Beneficial effects of Bacopa monnieri
958 extract on opioid induced toxicity. Heliyon 2, e00068.
959 Sheorey, R., Thangathiruppathy, A., Alagarsamy, V., 2016. Synthesis and Pharmacological Evaluation of 3-
960 propyl-2-substitutedamino-3H-quinazolin-4-ones as Analgesic and Anti-Inflammatory Agents. J.
961 Heterocycl. Chem. 53, 1371-1377.
962 Silva, R.H., Lima, N.d.F.M., Lopes, A.J., Vasconcelos, C.C., de Mesquita, J.W., de Mesquita, L.S., Lima, F.C.,
963 Ribeiro, M.N.d.S., Ramos, R.M., Cartágenes, M.d.S.d.S., 2017. Antinociceptive Activity of Borreria
964 verticillata: In vivo and In silico Studies. Front. Pharmacol. 8, 283.
965 Skidmore, I., Whitehouse, M., 1967. Biochemical properties of anti-inflammatory drugs—X: The inhibition
966 of serotonin formation in vitro and inhibition of the esterase activity of α-chymyotrypsin. Biochem.
967 Pharmacol. 16, 737-751.
968 Suba, V., Murugesan, T., Kumaravelrajan, R., Mandal, S.C., Saha, B., 2005. Antiinflammatory, analgesic and
969 antiperoxidative efficacy of Barleria lupulina Lindl. extract. Phytother. Res. 19, 695-699.

970 Systemes, D., 2015. BIOVIA, Discovery Studio Modeling Environment. Release 4.5. Dassault Systemes: San
971 Diego, CA.
972 Tjølsen, A., Berge, O.-G., Hunskaar, S., Rosland, J.H., Hole, K., 1992. The formalin test: an evaluation of the
973 method. Pain 51, 5-17.
974 Ullah, R., Ali, G., Subhan, F., Naveed, M., Khan, A., Khan, J., Halim, S.A., Ahmad, N., Al-Harrasi, A., 2021.
975 Attenuation of nociceptive and paclitaxel-induced neuropathic pain by targeting inflammatory, CGRP and
976 substance P signaling using 3-Hydroxyflavone. Neurochem. Int. 144, 104981.
977 Utsunomiya, I., Ito, M., Oh-ishi, S., 1998. Generation of inflammatory cytokines in zymosan-induced
978 pleurisy in rats: TNF induces IL-6 and cytokine-induced neutrophil chemoattractant (CINC) in vivo.
979 Cytokine 10, 956-963.
980 Van Hecke, O., Austin, S.K., Khan, R.A., Smith, B., Torrance, N., 2014. Neuropathic pain in the general
981 population: a systematic review of epidemiological studies. Pain 155, 654-662.
982 Wang, Y., Yu, C., Pan, Y., Li, J., Zhang, Y., Ye, F., Yang, S., Zhang, H., Li, X., Liang, G., 2011. A novel compound
983 C12 inhibits inflammatory cytokine production and protects from inflammatory injury in vivo. PLoS ONE
984 6, e24377.
985 Wisastra, R., Kok, P.A., Eleftheriadis, N., Baumgartner, M.P., Camacho, C.J., Haisma, H.J., Dekker, F.J., 2013.
986 Discovery of a novel activator of 5-lipoxygenase from an anacardic acid derived compound collection.
987 Bioorg. Med. Chem. 21, 7763-7778.
988 Yaouba, S., Koch, A., Guantai, E.M., Derese, S., Irungu, B., Heydenreich, M., Yenesew, A., 2018. Alkenyl
989 cyclohexanone derivatives from Lannea rivae and Lannea schweinfurthii. Phytochem. Lett. 23, 141-148.
990 Zanini Jr, J.C., Medeiros, Y.S., Cruz, A.B., Yunes, R.R., Calixto, J.B., 1992. Action of compounds from
991 Mandevilla velutina on croton oil-induced ear oedema in mice. A comparative study with steroidal and
992 nonsteroidal antiinflammatory drugs. Phytother. Res. 6, 1-5.

Maione, F., Colucci, M., Raucci, F., Mangano, G., Marzoli, F., Mascolo, N., Crocetti, L., Giovannoni, M.P., Di Giannuario, A., Pieretti, S., 2020. New insights on the arylpiperazinylalkyl pyridazinone ET1 as potent antinociceptive and anti-inflammatory agent. Eur. J. Pharmacol., 173572.

FIGURE LEGENDS:

Fig. 1. Chemical structure of Ethyl 6-(-4-methoxyphenyl)-2-oxo-4-phenylcyclohex-3-enecarboxylate

Fig. 2. Agarose gel electrophoresis (A) quantification of CHD activity on the mRNA level of COX-2 **(B)**, TNF-α **(C),** and IL-1β **(D)** in carrageenan induced hind paw edema in mice. The results are shown in relative arbitrary units (A.U). Bars represent mean expression in A.U ± S.E.M. ### $P < 0.001$ compared to the saline group. **$P < 0.01$, ***$P < 0.001$ compared to the vehicle group.

Fig. 3. Anti-nociceptive activity of (A) CHD and (B) the positive control, aspirin in the acetic acid (1%) induced abdominal constriction test. Each bar represents mean percentage protection ± S.E.M). *$P < 0.05$, **$P < 0.01$, ***$P < 0.001$ as compared to the saline treated group (one-way ANOVA followed by *post hoc* Dunnett's test), ($n = 6$ mice per group).

Fig. 4. Anti-nociceptive activity of CHD and the positive control, tramadol, in the hot-plate test. Each bar represents mean percentage protection ± S.E.M). *$P < 0.05$, **$P < 0.01$, ***$P < 0.001$ as compared to saline treated group (one-way ANOVA followed by *post hoc* Dunnett's test), ($n = 6$ mice per group).

Fig. 5. Anti-nociceptive activity of CHD and the positive control, tramadol in the thermal tail immersion test. Each bar represents mean withdrawal latency time in s ± S.E.M). *P< 0.05, **P< 0.01, ***P< 0.001 as compared to saline treated group (one-way ANOVA followed by *post hoc* Dunnett's test), (n = 6 mice per group).

Fig. 6. Anti-nociceptive activity of CHD and the positive controls, indomethacin (Indo), and diclofenac (Diclo) in the formalin induced paw nociceptive test. Each bar represents mean nociceptive response in s ± S.E.M). *P< 0.05, **P< 0.01, ***P< 0.001 as compared to the saline treated group (one-way ANOVA followed by *post hoc* Dunnett's test), (n = 6 mice per group).

Fig. 7. (A) Effect of naloxone at 1 mg/kg (NLX-1) and (B) PTZ at 15 mg/kg (PTZ-15) on the anti-nociceptive activity of CHD (30 mg/kg, CHD-30 and 45 mg/kg, CHD-45) or tramadol (30 mg/kg, TRD-30) in the mouse hot-plate test. Each bar represents mean percentage protection ± S.E.M. ***P < 0.001 compared to saline control (SAL). (two sample t-test), (n = 6 mice per group).

Fig. 8. Anti-inflammatory activity of (A) CHD and (B) the positive control, aspirin in the carrageenan induced paw edema test. Each bar represents paw volume in ml ± S.E.M. *P< 0.05, **P< 0.01, ***P< 0.001 as compared to saline treated group (one-way ANOVA followed by *post hoc* Dunnett's test), (n = 6 mice per group).

Fig. 9. Anti-inflammatory activity of (A) CHD and (B) the positive control, aspirin in the histamine induced paw edema test. Each bar represents paw volume in ml ± S.E.M. *P< 0.05, **P< 0.01, ***P< 0.001 as compared to saline treated group (one-way ANOVA followed by *post hoc* Dunnett's test), (n = 6 mice per group).

Fig. 10. Anti-inflammatory activity of (A) CHD and (B) the positive control, aspirin in the serotonin induced paw edema test. Each bar represents paw volume in ml ± S.E.M. *P< 0.05, **P< 0.01, ***P< 0.001 as compared to saline treated group (one-way ANOVA followed by *post hoc* Dunnett's test), (n = 6 mice per group).

Fig. 11. Anti-inflammatory activity of CHD and the positive controls, indomethacin (Indo), and diclofenac (Diclo) in the xylene induced ear edema test. Each bar represents ear weight in mg ± S.E.M. **P*< 0.05, ***P*< 0.01, ****P*< 0.001 compared to the saline treated group (one-way ANOVA followed by *post hoc* Dunnett's test), (*n* = 6 mice per group).

Fig. 12. (A) Ribbon diagram of overlaid binding orientation of CHD and native ligand into the binding site of the COX-2 enzyme. **(B)** Three-dimensional ligand-enzyme interaction plots of the cyclohexenone derivative (CHD) into the binding site of COX-2 enzyme

Fig. 13. (**A**) Three-dimensional superimposed binding pose of the native ligand benzamidine (yellow), cyclohexenone derivative (CHD; purple) and methaqualone (orange) into the binding site of the $GABA_A$ receptor (PDB code 4COF) and (**B**) Two-dimensional interaction plot for CHD.

Fig. 14. Three and Two dimensional models of CHD binding with opioid receptors. **(A**) Three-dimensional and (**B)** Two-dimensional modeled superimposed binding pose of native ligand and CHD (purple) into the binding site of δ-opioid receptors (PDB code = 4EJ4). (**C)** Three-dimensional and **(D)** Two-dimensional model superimposed binding pose of native ligand and CHD (purple) into the binding site of κ-opioid receptor (PDB code = 4DJH). (**E**) Three-dimensional and (**F**) Two-dimensional model superimposed binding pose of the native ligand and selected compound CHD (purple) into the binding site of μ-opioid receptors (4DKL).

Fig. 15. (**A**) Root Mean Square Devitaions of backbone atoms for each receptor of docked complexes. (**B**) CHD Root Mean Square Devitaions over 50-ns of MD simulation in complex with receptors.